Comparison of geodetic and geologic data from the Wasatch region, Utah, and implications for the spectral character of Earth deformation at periods of 10 to 10 million years

Anke M. Friedrich,[1] Brian P. Wernicke, and Nathan A. Niemi[2]
Division of Geological and Planetary Sciences, California Institute of Technology, Pasadena, California, USA

Richard A. Bennett and James L. Davis
Smithsonian Astrophysical Observatory, Harvard University, Cambridge, Massachusetts, USA

Received 22 June 2001; revised 2 June 2002; accepted 21 November 2002; published 15 April 2003.

[1] The Wasatch fault and adjacent fault zones provide an opportunity to compare present-day deformation rate estimates obtained from space geodesy with geologic displacement rates over at least four temporal windows, ranging from the last millennium up to 10 Myr. The three easternmost GPS sites of the Basin and Range Geodetic Network (BARGEN) at this latitude define a ~130-km-wide region spanning three major normal faults extending east-west at a total rate of 2.7 ± 0.4 mm/yr, with an average regional strain rate estimated to be 21 ± 4 nstrain/yr, about twice the Basin and Range average. On the Wasatch fault, the vertical component of the geologic displacement rate is 1.7 ± 0.5 mm/yr since 6 ka, <0.6 mm/yr since 130 ka, and 0.5–0.7 mm/yr since 10 Ma. However, it appears likely that at the longest timescale, rates slowed over time, from 1.0 to 1.4 mm/yr between 10 and 6 Ma to 0.2 to 0.3 mm/yr since 6 Ma. The cumulative vertical displacement record across all three faults also shows time-variable strain release ranging from 2 to 4 mm/yr since 10 ka to <1 mm/yr averaged over the past 130 kyr. Conventional earthquake recurrence models (''Reid-type'' behavior) would require an accordingly large variation in strain accumulation or loading rate on a 10-kyr timescale, for which there appears to be no obvious geophysical explanation. Alternatively, seismic strain release, given a wide range of plausible constitutive behaviors for frictional sliding, may be clustered on the 10-kyr timescale, resulting in the high Holocene rates, with comparatively low, uniform strain accumulation rates on the 100-kyr timescale (''Wallace-type'' behavior). The latter alternative, combined with observations at the million-year timescale and the likelihood of a significant contribution of postseismic transients, implies maxima of spectral amplitude in the velocity field at periods of ~10 Myr (variations in tectonic loading), ~10 kyr (clustered strain release), and of 100 years (postseismic transients). If so, measurements of strain accumulation and strain release may be strongly timescale-dependent for any given fault system. *INDEX TERMS:* 1208 Geodesy and Gravity: Crustal movements—intraplate (8110); 1243 Geodesy and Gravity: Space geodetic surveys; 7209 Seismology: Earthquake dynamics and mechanics; 8107 Tectonophysics: Continental neotectonics; 8109 Tectonophysics: Continental tectonics—extensional (0905); *KEYWORDS:* geodetic, geologic, fault slip rate, normal fault, timescale, earthquake cycle

Citation: Friedrich, A. M., B. P. Wernicke, N. A. Niemi, R. A. Bennett, and J. L. Davis, Comparison of geodetic and geologic data from the Wasatch region, Utah, and implications for the spectral character of Earth deformation at periods of 10 to 10 million years, *J. Geophys. Res.*, *108*(B4), 2199, doi:10.1029/2001JB000682, 2003.

1. Introduction

[2] Geodetic data and geological displacement rate data are the observational basis for physical models of the earthquake deformation cycle and the assessment of seismic hazards. In the simplest model, the elastic strain energy accumulated across locked faults is periodically released during earthquakes of relatively uniform slip and recurrence interval, each of which releases the strain energy accumulated since the last earthquake (Figure 1a) [*Reid*, 1910; *Savage and Burford*, 1973; *Scholz*, 1990]. In this model, far-field displacement, which is proportional to strain accumulation, occurs at a uniform rate and is equal to the displacement rate recorded by earthquakes on the fault.

[1]Now at Institute of Geosciences, Potsdam University, Golm, Germany.
[2]Now at Institute for Crustal Studies, University of California, Santa Barbara, California, USA.

0148-0227/03/2001JB000682$09.00

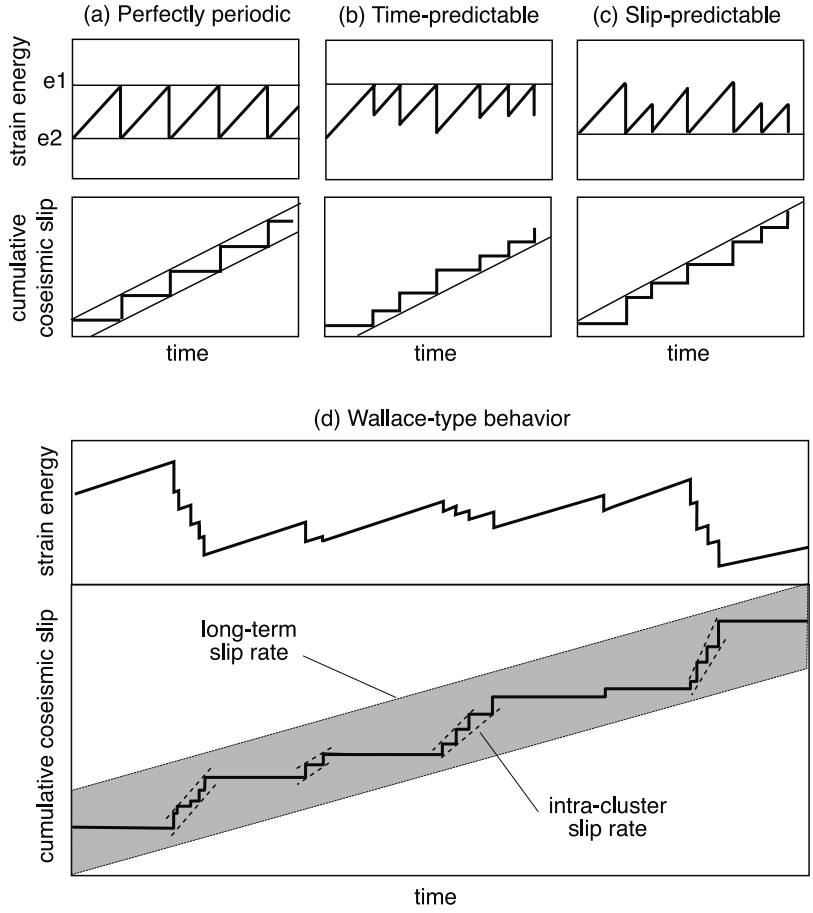

Figure 1. Strain release models for earthquakes (Figures 1a–1c are redrawn after *Scholz* [1990]). (a) Perfectly periodic model [*Reid*, 1910], (b) time-predictable model where the size of the last earthquake predicts the time of the next earthquake [*Shimazaki and Nakata*, 1980], and (c) slip-predictable model where the time since the last earthquake predicts the size of the next earthquake [e.g., *Shimazaki and Nakata*, 1980]. (d) Clustered strain release and uniform, low strain accumulation, modified after *Wallace* [1987]. See color version of this figure in the HTML.

This model was modified to account for the fact that the interseismic interval and the size of earthquakes on a particular fault are not perfectly periodic [e.g., *Shimazaki and Nakata*, 1980]. One variant is the "time-predictable" model where each event occurs when a critical amount of strain energy has accumulated (Figure 1b). In this model, the slip rate and the size of the last earthquake predict the time, but not the size, of the next earthquake. Another variant is the "slip-predictable" model where for any given event, all strain energy accumulated since the last earthquake is released. In this model, the slip rate and the time since the last earthquake are combined to predict the size, but not the time, of the next event (Figure 1c).

[3] In terms of both earthquake physics and hazards analysis, models such as these beg the question [*Wallace*, 1987; *Ward*, 1998]: Is the strain release rate of some small number of earthquakes equal to the long-term strain accumulation rate applied to faults? All three models assume a constant rate of far-field displacement and strain accumulation, and therefore predict that well-constrained slip histories, determined over several earthquake cycles, will agree with contemporary interseismic measurements of far-field displacement. The question is complicated, however, by the fact that it is not clear to what degree both strain accumulation and release are influenced by local stress diffusion within a viscous or viscoelastic substrate due to each event [e.g., *Foulger et al.*, 1992; *Hager et al.*, 1999; *Kenner and Segall*, 2000; *Wernicke et al.*, 2000]. Here we evaluate these issues through comparison of recently acquired geodetic data with displacement rates derived from paleoseismic and other geologic data for the Wasatch and related faults, which are among the best characterized Quaternary fault systems in the world [e.g., *Machette et al.*, 1992a].

[4] For the Wasatch and a number of other fault zones, an important consideration in comparing deformation rates on different timescales is that strain release may occur during "clusters" of earthquakes, wherein recurrence intervals are as much as an order of magnitude shorter than during quiescent periods between clusters [*Wallace*, 1987; *Swan*, 1988; *Sieh et al.*, 1989; *McCalpin and Nishenko*, 1996; *Grant and Sieh*, 1994; *Marco et al.*, 1996; *Zreda and Noller*, 1998; *Rockwell et al.*, 2000]. Clustering is consistent with the time-predictable and slip-predictable behavior. However, because slip per event for most well-documented fault segments does not appear to be highly variable [e.g., *Schwartz and Coppersmith*, 1984], these models require

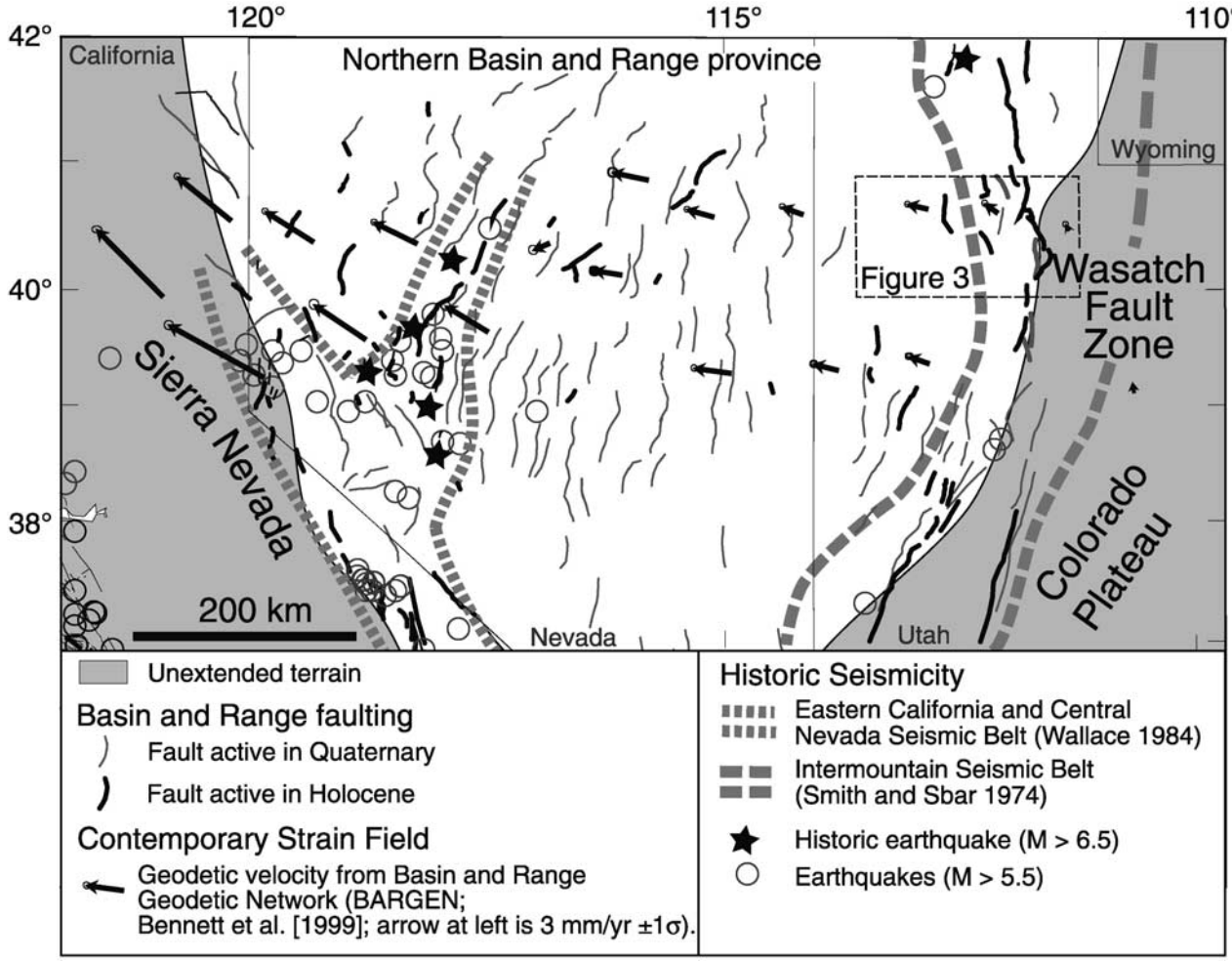

Figure 2. Simplified tectonic map of the northern Basin and Range province, located between the Sierra Nevada and the Colorado plateau. The BARGEN geodetic velocities [e.g., *Bennett et al.*, 1999] and the distribution of active normal faults and historic earthquakes are shown. See color version of this figure in the HTML.

that strain accumulation (via changes in either the far-field or local processes mentioned above) would vary markedly, on the same timescale as the clusters. In this event, at any given time strain accumulation inferred from geodesy and strain release inferred from paleoseismology should be the same. On the other hand, far-field strain accumulation may be constant, generally being lower than seismic strain release rates during clusters, and higher in between clusters. In this case, strain release would bear no relation to either a critical level of strain energy required for slip (time-predictable model), nor the amount of strain energy accumulated since the previous earthquake (slip-predictable model) (Figure 1d) [*Wallace*, 1987].

[5] The Wasatch fault zone is ideally suited for comparisons of strain accumulation and release because the slip histories of most or all segments of the fault are well known, and there are good constraints on the longer term slip history [e.g., *Machette et al.*, 1992a, 1992b; *McCalpin and Nishenko*, 1996; *McCalpin and Nelson*, 2000; *Parry and Bruhn*, 1987; *Ehlers et al.*, 2001]. In this paper we present new geodetic data from the Basin and Range Geodetic Network (BARGEN) from 1996 to 2000 across the eastern Basin and Range-Colorado Plateau transition region at the latitude of Salt Lake City and compare them with a synthesis of published geological displacement rates across the same region at the 1-kyr, 100-kyr, 1-Myr, and 10-Myr timescales.

2. Neotectonic Setting

[6] The northern Basin and Range province, bounded on the west by the Sierra Nevada and on the east by the Colorado Plateau (Figure 2), is a wide (~750 km) region of extended continental crust. Extension initiated in the Oligocene and peaked during mid to late Miocene time (~15–10 Ma [*Stockli*, 2000]) with a maximum displacement rate near 20 mm/yr [*Wernicke and Snow*, 1998], resulting in the formation of range front faults spaced ~30 km apart, separating ~15-km-wide basins from mountain ranges. Since ~10 Ma the overall rate of deformation has slowed to about half the maximum value and includes a major component of right-lateral shear along the western margin of the province [*Bennett et al.*, 1998, 1999; *Thatcher et al.*, 1999].

[7] Most range-bounding faults in Nevada and western Utah have been active in Quaternary time [*Dohrenwend et al.*, 1996; *Hecker*, 1993]. Regions of modern seismicity, however, are restricted to three narrow belts, the Eastern

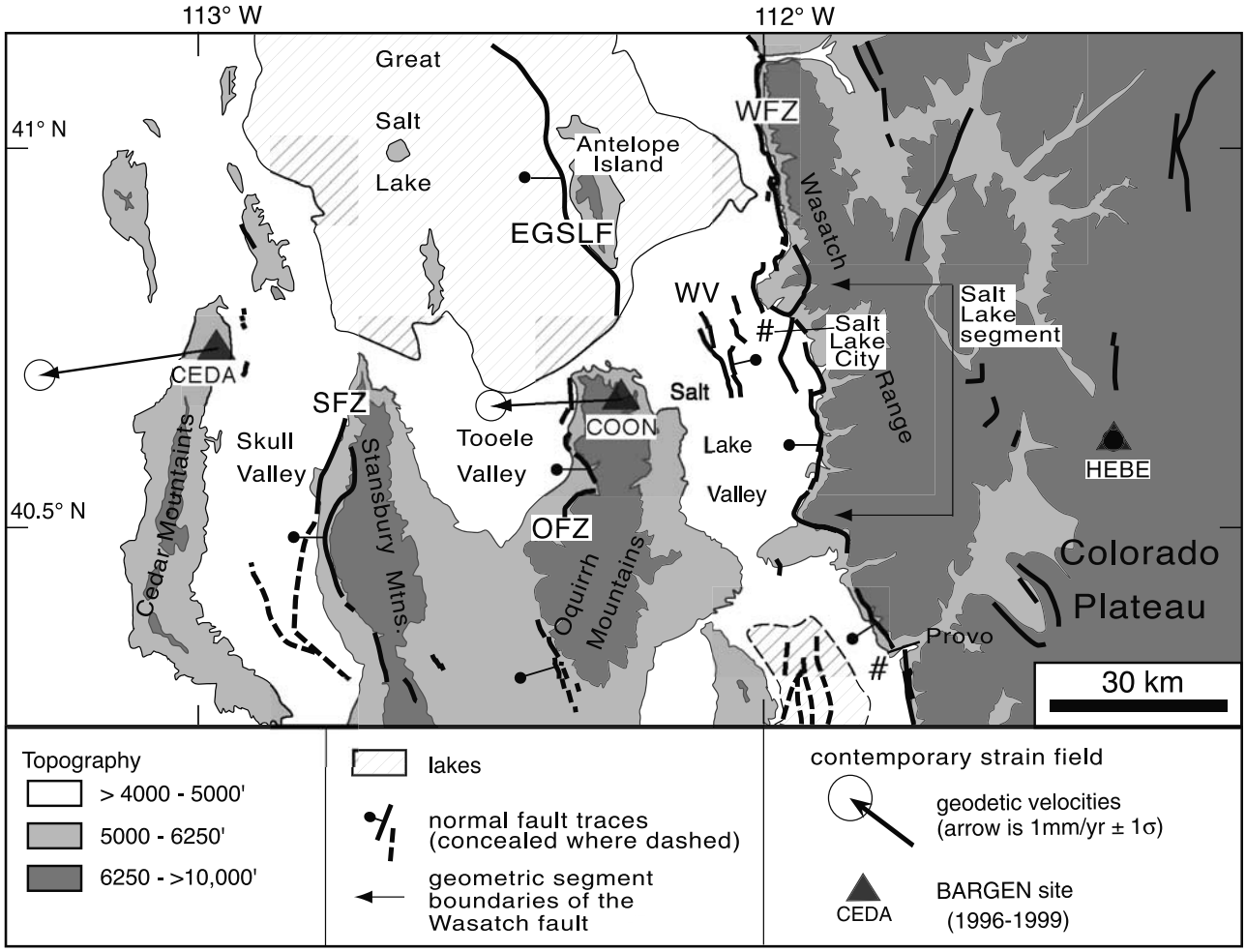

Figure 3. Simplified tectonic map of the Wasatch, West Valley, Oquirrh, and Stansbury faults, showing present-day basin and range topography, and locations of BARGEN GPS sites with velocity relative to site HEBE [e.g., *Bennett et al.*, 1999]. WFZ, Wasatch fault zone; WV, West Valley fault zone; EGSL, East Great Salt Lake fault zone; OFZ, Oquirrh fault zone; SFZ, Stansbury fault zone. See color version of this figure in the HMTL.

California, Central Nevada, and Intermountain Seismic Belts, which also comprise the locations of significant (M > 6.5) historic earthquakes (Figure 2) [*Smith and Sbar*, 1974; *Wallace*, 1984]. Only one of these, the 1934 Hansel Valley earthquake in northernmost Utah, occurred in the Intermountain Seismic Belt [*Doser*, 1989]. The most recent earthquake on the Salt Lake segment of the Wasatch fault occurred at ~1.3 ka (Figure 3) [*Black et al.*, 1996; *McCalpin and Nishenko*, 1996]. However, an even more recent event occurred ~400 years ago on the East Great Salt Lake fault (Figure 3), the first major fault zone to the west of the Wasatch fault [*Dinter and Pechmann*, 1999; D. Dinter and J. Pechman, personal communication, 2001].

2.1. Regional Setting and Fault Geometry

[8] The largest normal fault of the Intermountain Seismic Belt at 40.5°N latitude is the >350-km-long Wasatch fault which consists of 10 segments defined on the basis of their geometry [e.g., *Machette et al.*, 1991, 1992a, 1992b]. The central segments define a sharp boundary between the Basin and Range province and the unextended Colorado Plateau (Figures 2 and 3). The BARGEN geodetic sites HEBE and COON span a baseline across the Salt Lake segment of the Wasatch fault, which consists of the main range-bounding fault and a pair of east dipping faults (collectively, the West Valley faults) that are exposed in the center of sediment-filled Salt Lake Valley (Figure 3). The footwall of the Wasatch fault, the Wasatch Range, comprises a thrust stack formed during the Late Cretaceous Sevier orogeny, when Proterozoic basement and Paleozoic sedimentary rocks were thrust eastward over Mesozoic foreland rocks [e.g., *DeCelles et al.*, 1995]. Early to mid-Tertiary sedimentary and volcanic rocks unconformably overlie pre-Tertiary strata along the east flank of the Wasatch Range (Figure 4) [*Bryant*, 1990, 1992]. Subsequent to deposition of these strata, the range was tilted eastward 20°–30°, resulting in ~11 km of footwall exhumation [e.g., *Parry and Bruhn*, 1987; *Wernicke and Axen*, 1988].

[9] The subsurface geometry of the Wasatch fault is constrained by structural, gravity, borehole, and seismic reflection data, but there is nonetheless no clear indication as to its average dip through the seismogenic crust. Near-surface fault dips range from 30° to 70° [*Smith and Bruhn*, 1984; *Bruhn et al.*, 1992], whereas seismic reflection data

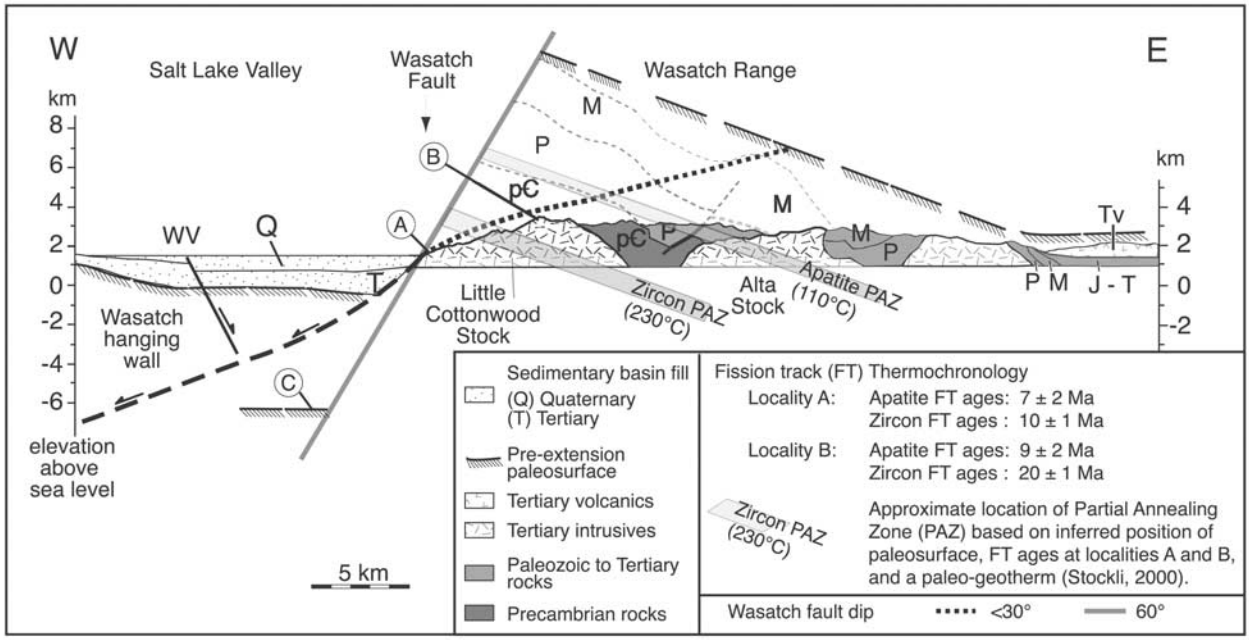

Figure 4. Simplified structural section across the Wasatch Range and Salt Lake Valley modified after Figure 3 of *Parry and Bruhn* [1987]. See text for discussion. Q, Quaternary deposits; T, Tertiary sediments in Salt Lake Valley; Tv, Tertiary volcanic rocks; J-T, Jurassic to Tertiary sedimentary rocks; M, Mesozoic; P, Paleozoic; p-C, Proterozoic rocks; WV, West Valley fault zone. See color version of this figure in the HTML.

across fault segments to the north and south of the study region indicate much lower dips (<30°) at shallow depths (1–4 km) [*Smith and Bruhn*, 1984]. The sedimentary fill in Salt Lake Valley is less than 2 km thick at its deepest locality (Figure 4) [e.g., *Arnow and Mattick*, 1968; *Keaton et al.*, 1987]. Compared with the exhumation record of the Wasatch footwall (Appendix A), the relatively small volume of sediments in hanging wall basins implies that most of the exhumation occurred by tectonic rather than erosional denudation. On the basis of the amount of basin fill and the projected position of the preextension paleosurface, we infer an average initial dip of ~20°–30° (Figure 4), which would imply that the active trace at depth has a similar average dip, depending on the amount of tilt of the fault plane due to slip. Such a low dip angle is consistent with seismic reflection data for the Weber and Levan segments, which lie north and south of the Salt Lake segment, respectively [*Smith and Bruhn*, 1984]. However, the active trace may not be the same fault that unroofed the Wasatch footwall. Therefore the existing data are inconclusive as to the average dip of the active trace through the upper crust, which in any event may be strongly variable along strike.

[10] Two major normal fault systems to the west of the Wasatch fault, the Oquirrh-East Great Salt Lake and Stansbury faults (Figure 3), are generally similar to the Wasatch fault, although the total displacement across these faults is probably less. The west dipping Oquirrh-East Great Salt Lake fault separates Proterozoic-Paleozoic rocks of Antelope Island and the Oquirrh Mountains from Quaternary-Tertiary basin fill up to 4 km thick with an estimated throw of at least 6 km [e.g., *Viveiros*, 1986]. The Oquirrh fault dips 50°–70° at the surface [*Lee and Bruhn*, 1996], but seismic reflection data for the East Great Salt Lake fault [*Smith and Bruhn*, 1984; *Viveiros*, 1986; *Pechmann et al.*, 1987] and gravity data for the hanging wall basin [*Cook et al.*, 1966] suggest a low-angle dip (~30° or less) at only a few kilometers depth. Although fault dips near 30° are not uncommon for normal faults across west central Utah, including the Sevier Desert region where they have been clearly imaged in seismic reflection profiles [e.g., *Allmendinger et al.*, 1983], the dips of both the Oquirrh, Stansbury and related faults are poorly constrained.

[11] The west dipping Stansbury normal fault system is comprised of two main range-bounding fault segments and two faults farther west, in Skull Valley, with a total estimated vertical offset of 5 km (Figure 3) [*Helm*, 1995; *Hanson*, 1999]. Similar to the Salt Lake segment of the Wasatch fault, the depth of Quaternary basin fill is ~2 km, and the amount of tilt of both hanging wall and footwall range blocks is ~20° [*Hanson*, 1999].

3. Contemporary Horizontal Velocity Field

[12] We determined the present-day horizontal velocity field across the Wasatch, Oquirrh, and Stansbury Mountains and adjacent areas of Utah and Nevada using daily Global Positioning System (GPS) position estimates for BARGEN sites between latitudes 39°N and 40°N from August 1996 through November 2000. The key sites for this study include HEBE, COON, CEDA, GOSH, and RUBY (Figures 3 and 5 and Table 1) [*Bennett et al.*, 1998, 1999, 2003]. The GPS monuments are anchored into bedrock to a depth of 10 m to minimize any errors due to nontectonic motions near the Earth's surface [e.g., *Langbein et al.*, 1995]. Daily horizontal position estimates are repeatable at the 2 mm level or better [*Wernicke et al.*, 2000; *Davis et al.*, 2003].

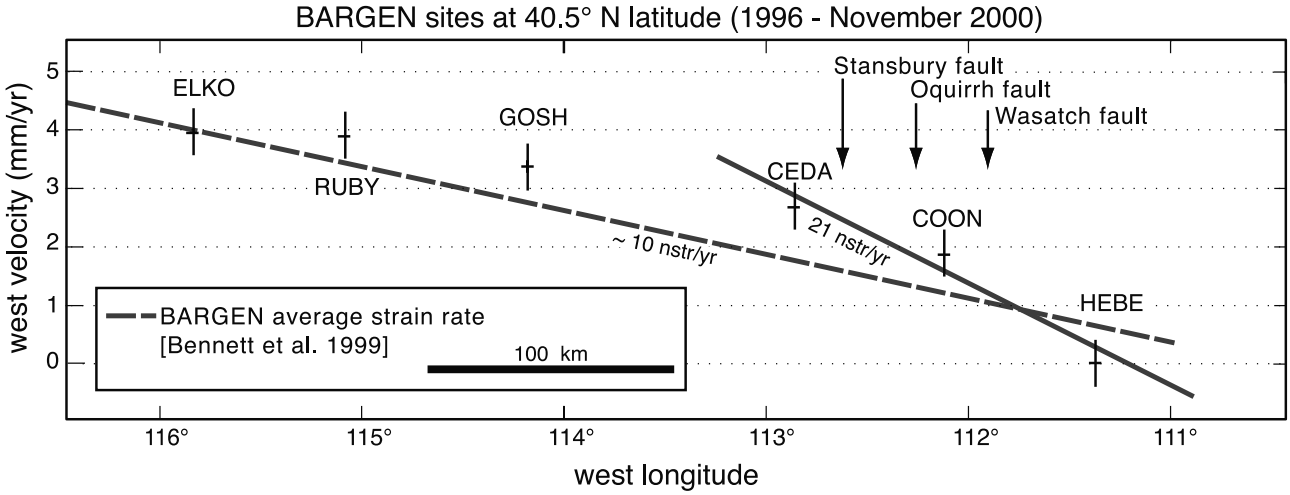

Figure 5. Diagram of west velocity versus position for BARGEN sites across the Wasatch fault and surrounding faults. The dashed line shown for comparison is the average Basin and Range strain rate determined by all BARGEN sites at this latitude [*Bennett et al.*, 1999; *Wernicke et al.*, 2000]. Uncertainties are shown at 95% confidence [e.g., *Davis et al.*, 2003]. See color version of this figure in the HTML.

The velocity field determined using least squares techniques (as described by *Bennett et al.* [1999, 2003]) yield uncertainties in the 0.1 mm/yr range (Figure 3). However, the observed scatter in velocity components with respect to position relative to simple linear regressions [*Davis et al.*, 2003] suggests a more conservative estimate of 0.2 mm/yr for the total 1σ error in velocity, which we will adopt in considering regional strain rates (Table 1 and Figure 5).

[13] The overall velocity field for the eastern Great Basin suggests uniaxial east-west extension, with west components of motion generally increasing westward from the Colorado Plateau, and north components not significantly different from zero. Linear regression of the west components with respect to longitude yields an average strain rate for the eastern Great Basin of ~10 nstrain/yr [*Bennett et al.*, 1999]. However, the gradient in west velocity appears to be higher for sites east of CEDA than for those to the west. Regression of the west components of velocity with respect to position for HEBE, COON, and CEDA (assigning a velocity error for HEBE commensurate to the other two sites) yields a strain rate of 21 ± 4 nstrain/yr across the 130-km-wide region.

[14] The 65-km baseline spanning the Wasatch fault, HEBE-COON, is extending at 1.9 ± 0.2 mm/yr (1σ, or 28 ± 3 nstrain/yr. This baseline spans an earlier network surveyed by ground-based techniques [*Savage et al.*, 1992] and campaign mode GPS [*Martinez et al.*, 1998]. Trilateration surveys from 1970 to 1990 indicated an east-west elongation rate of 47 ± 11 nstrain/yr (1σ), the GPS surveys from 1992 to 1995 indicated a rate of 49 ± 23 nstrain/yr, and a combined analysis of all ground- and space-based surveys (1962–1994) yielded a rate of 51 ± 9 nstrain/yr [*Martinez et al.*, 1998, Table 1]. Our results are therefore consistent with the campaign GPS results alone (which are barely significant at 2σ) and marginally consistent with the ground-based and combined solutions near their lower limits at two standard deviations.

4. Synthesis of Vertical Displacement History

[15] Displacement rates on normal faults may be determined by various methods across a wide range of timescales (Table 2). Fault scarps often form within late Quaternary alluvial, lacustrine, or glacial deposits, and may be preserved for hundreds of thousands of years (Figure 6). On the Holocene/latest Pleistocene timescale (~0.1 to ~25 ka; Figure 7), fault displacement rates are typically determined by paleoseismic methods, which may reveal the detailed earthquake time series and displacement history for a number of earthquakes on a fault (Table 2). Immediately after an earthquake, an apron of debris, or colluvial wedge,

Table 1. Geodetic Velocities of Basin and Range Geodetic (BARGEN) Sites in the Eastern Basin and Range, Utah, Recorded Between 1996 and November 2000

Site	Longitude, deg	Latitude, deg	West Velocity,[a] mm/yr	North Velocity,[a] mm/yr	1σ West Uncertainty, mm/yr	1σ North Uncertainty, mm/yr
ELKO	244.183	40.915	3.98	−0.3	0.2	0.2
RUBY	244.877	40.617	2.2	−0.5	0.2	0.2
GOSH	245.820	40.640	3.4	−0.7	0.2	0.2
CEDA	247.140	40.681	2.7	−0.4	0.2	0.2
COON	247.879	40.653	1.9	−0.1	0.2	0.2
HEBE	248.627	40.514	0	0	0.2	0.2

[a]The velocities are given with respect to site HEBE. The west and north velocity components of HEBE relative to a North American reference frame are 0.26 ± 0.08 and 0.66 ± 0.07 mm/yr (1σ), respectively. See *Bennett et al.* [2003] for details.

Table 2. Significance of Present-Day and Geologic Displacement Rate Measurements on Normal Faults

Method	Time Interval	What Is Measured? (Typical Units)	Significance of Measurements
Geodetic	hours to years	horizontal velocity field or strain rate (mm/yr or nstrain/yr)	Far-field (tectonic) strain accumulation Postseismic viscoelastic relaxation
Paleoseismic	10^1 to 10^4 years	earthquake recurrence interval (ka); net vertical tectonic displacement record (m)	strain release rate via individual earthquakes and clusters
Geomorphic	10^3 to 10^6 years	vertical displacement (m) and age of offset marker horizon (ka) yield vertical displacement rate (m/kyr)	average fault displacement rates of a number of seismic cycles
Geologic/Structural	10^6 to 10^7 years	horizontal and vertical displacement rate (km/Myr)	average tectonic fault displacement rates (km/Myr)
Thermochronologic	10^6 to 10^7 years	crustal cooling rates (°C/Myr)	exhumation rates (km/Myr)

begins forming on the hanging wall adjacent to the scarp [e.g., *Machette et al.*, 1992a, 1992b; *Nelson*, 1992; *McCalpin and Berry*, 1996]. The timing of an earthquake may be constrained by dating "event horizons," such as the base of the colluvial wedge. Alternatively, deposits that entomb the colluvial wedge may also provide a relatively tight constraint [e.g., *Nelson*, 1992; *McCalpin and Nishenko*, 1996]. The amount of displacement during an event is generally difficult to constrain due to uncertainties in the geometry of the fault plane itself. However, offset horizons traceable across the fault zone generally permit an accurate determination of the vertical component of displacement (net vertical tectonic displacement or NVTD [*Witkind*, 1964; *Crone et al.*, 1987; *Caskey et al.*, 1996]).

[16] On the 100-kyr timescale (>50 kyr to hundreds of thousands of years), offset features, such as alluvial, glacial, or lacustrine horizons do not yield time series of earthquakes, but may yield accurate displacement rates averaged over many seismic cycles (Table 2). The accuracy of 100-kyr-scale displacement rates depends on unambiguous identification of offset marker units, and the availability of absolute ages of offset surfaces or deposits. These marker units are most commonly soils developed on top of glacial, lacustrine, and alluvial deposits. In the desert southwest, direct age constraints on these surfaces are generally lacking, but it is possible to bracket their time of development by placing them in the context of late Pleistocene glaciations, whose ages may be estimated using the global marine oxygen isotopic record [e.g., *Imbrie et al.*, 1984; *Machette*, 1981; *Bull*, 2000]. Glacial periods are marked by the deposition of till, lacustrine sedimentation, and the aggradation of alluvial fans. Interglacial periods, in contrast, tend to be marked by the development of soil horizons on these deposits [e.g., *Machette*, 1981]. Therefore, if a surface can be assigned unambiguously to a particular interglacial interval, then its age is bracketed by the duration of the isotopic excursion that defines the interglacial interval (Figure 7). For most of the three intervals prior to the current interglacial, the uncertainty in age, and therefore displacement rate, is on the order of 30–50%. Even if a given deposit cannot be unambiguously correlated with the global marine record, it may still provide useful limits on displacement rates.

[17] On the million-year timescale (~1 to >15 Ma), average displacement rates are inferred from thermochronologic, thermobarometric, and structural methods (Table 2). Uncertainties in vertical displacement rates derived from thermochronology depend on knowledge of the paleothermal structure of the crust, the analytical uncertainties in fission track ages (~10%, 2σ [*Dimitru*, 2000]), fault geometry, and location of the paleosurface (e.g., Figure 4 and Appendix A). Below we summarize published fault displacement data at each timescale.

4.1. Thousand-Year Timescale (Holocene/Latest Pleistocene)

[18] Faulting since the last glacial interval (24–12 ka) is well recorded in abundant lacustrine deposits throughout the region related to Lake Bonneville and glacial deposits along the Wasatch front (Figure 6) [e.g., *Scott et al.*, 1983]. The presence of former Lake Bonneville is manifested by the onset of filling at ~26 ka, and three prominent highstand shorelines, the Bonneville (~17 ka), Provo (~14 ka), and Gilbert (~13 ka) (Figures 6 and 7) [*Oviatt et al.*, 1992]. The oldest faulting events may be distinguished based on whether or not they cut deposits associated with the onset of filling or with these shorelines. The ages and amounts of displacement for most recorded events, however, are derived from post-Gilbert colluvial wedges documented in trenches.

4.1.1. Wasatch Fault Zone

[19] Mid to late Holocene vertical displacement rates across the Wasatch fault, except for its southernmost segment, range from 1.0 to 1.7 mm/yr (Figure 8). On the basis of paleoseismic studies in a number of trenches along the Salt Lake segment [*Swan et al.*, 1980; *Black et al.*, 1996], four Holocene earthquakes with NVTDs of 2–2.5 m have occurred since 6 ka, yielding an average vertical displacement rate we estimate to be 1.7 ± 0.5 mm/yr (Figure 8a).

[20] The longest time series of earthquakes on the Salt Lake segment is derived from a "megatrench" excavated across alluvial and lacustrine deposits in the vicinity of Little Cottonwood Canyon (Figure 6) [*McCalpin and Nelson*, 2000; *McCalpin*, 2002]. In addition to the four events known from the other trenches (Z, Y, X, and W, Figure 8a), they documented two additional events between 7 and 10 ka (V and U, Figure 8a). However, on the same scarp, only one event (T, Figure 8a) is observed between 10 ka and the onset of Bonneville sedimentation at 26 ka. Given this time series, the average Holocene recurrence interval is ~1.7 kyr, whereas the two pre-Holocene interseismic intervals are 7 kyr and at least 10 kyr, about a factor of 4–5 longer than for the Holocene.

[21] The partitioning of NVTDs among the pre-6 ka events are not well constrained. However, deposits of the

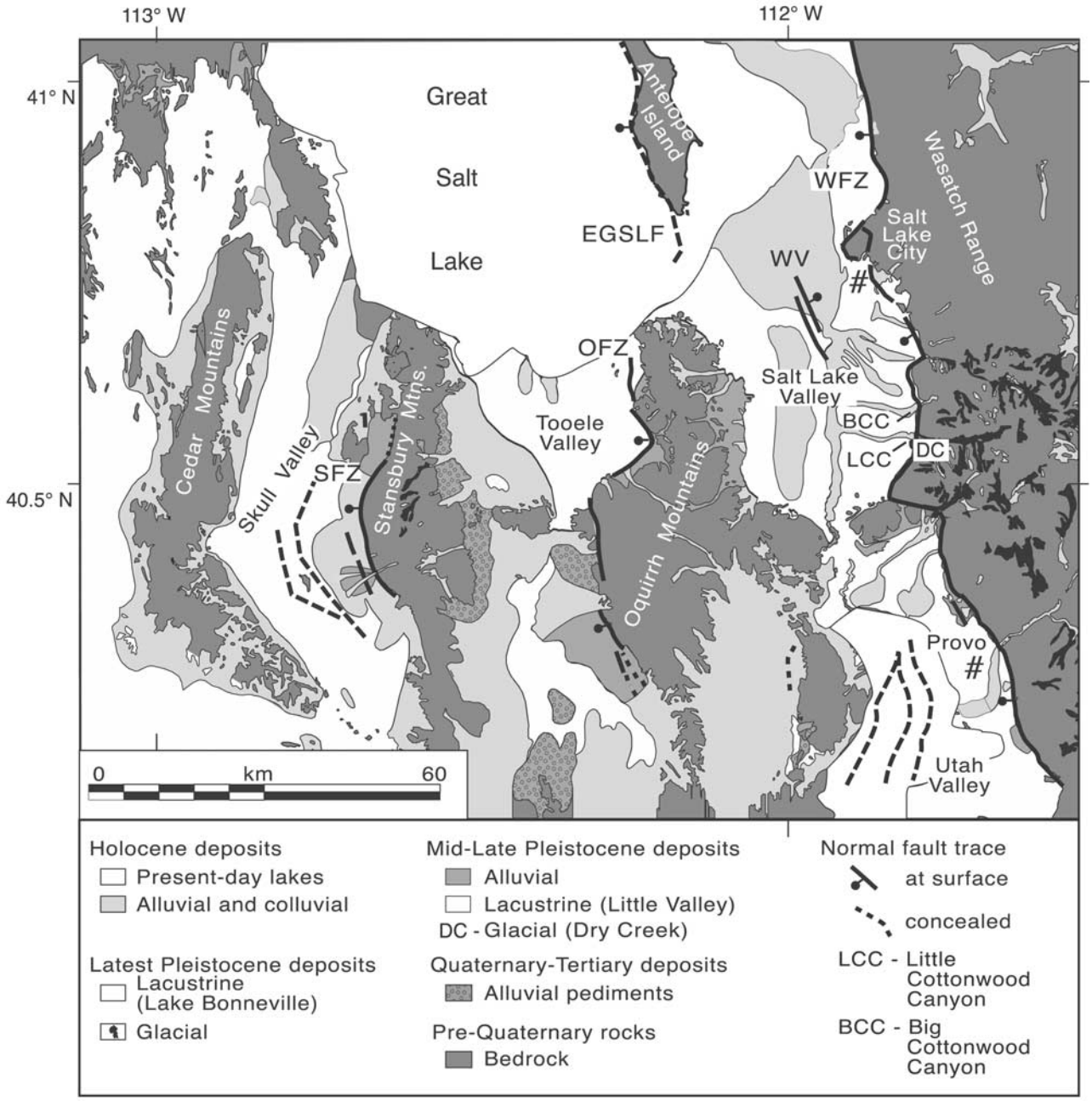

Figure 6. Simplified neotectonic map of the Salt Lake City region showing the distribution of Quaternary deposits from which fault slip data were compiled. Fault displacement rates in Mid-Pleistocene deposits can only be determined in limited regions where the younger Lake Bonneville deposits are topographically below the fault trace. See color version of this figure in the HMTL.

Lake Bonneville highstand (~17 ka) are offset a total of 18.3 m [*McCalpin and Nelson*, 2000], yielding an average vertical displacement rate of ~1 mm/yr. Of this amount, at least 7 m and as much as 12 m of displacement is attributed to the four most recent events, although this amount is a maximum for the NVTD because the trench did not extend across antithetic faults farther west [*McCalpin and Nelson*, 2000]. Near the megatrench, the Bell Canyon moraine (Figures 6 and 7b) is offset by ~14 m, which combined with its recently revised age of ~14 to 15 ka, yields a vertical displacement rate of ~1 mm/yr [*Scott and Shroba*, 1985; *Schwartz and Lund*, 1988; E. Lips, personal communication, April 2001]. These offsets suggest events V, U, and T have an average NVTD similar to those of the younger four events. If so, then the total NVTD of ~3 m between 26 and 10 ka yields an average vertical displacement rate of ~0.2 mm/yr, about an order of magnitude lower than the rate since 6 ka.

4.1.2. West Valley Fault Zone

[22] The latest Pleistocene/Holocene displacement rate across the two east dipping fault splays in Salt Lake Valley is similar to that of the Wasatch fault. The NVTD across the

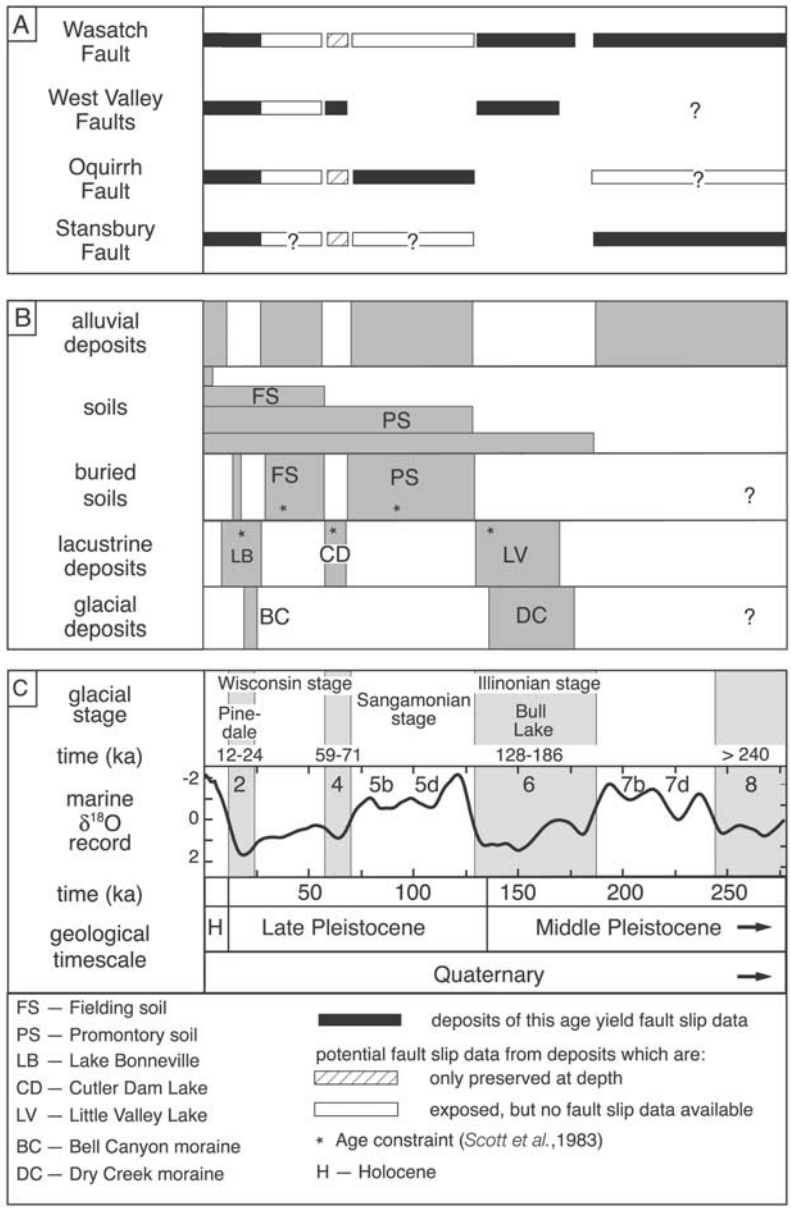

Figure 7. Correlation diagram of Late Quaternary deposits in the Wasatch region. (a) Time intervals (black bars) upon which displacement rate data have been published. Additional displacement rate data may be obtained for the time intervals shown by white and hatched boxes. (b) Estimated age distribution for each type of deposit, based on published data [e.g., *Scott et al.*, 1983; *Scott*, 1988; *Machette*, 1981; *Machette et al.*, 1992b]. (c) Timescale diagram showing the North American Glacial Stages, glacial deposits of the Rocky Mountain region, and marine oxygen isotope record [e.g., *Imbrie et al.*, 1984; *Richmond*, 1986]. See color version of this figure in the HTML.

West Valley faults has been approximately 8 ± 1 m since 13 ka, yielding an average vertical displacement rate of 0.5–0.6 mm/yr, whereas faulting occurred at a much lower rate in the late Pleistocene (Figure 8b) [*Keaton et al.*, 1987]. The last two events occurred shortly after 3.4 ka and at ~2.3 ka [*Solomon*, 1998], but the detailed displacement history since 13 ka is poorly constrained.

4.1.3. Oquirrh Fault Zone

[23] Lake Bonneville sediments were offset ~6 to 8 m by the northern Oquirrh fault in three events at 6.5 ± 1.5 ka, 23 ± 3 ka, and prior to 34 ka (Figure 8c) [*Olig et al.*, 1994], yielding a maximum vertical displacement rate of 0.20 ± 0.05 mm/yr since 34 ka [*Olig et al.*, 1994].

4.1.4. Stansbury Fault Zone

[24] Holocene/Latest Pleistocene faulting across the Stansbury fault zone occurred on several fault splays. The main range-bounding fault yields a NVTD of ~11 m in the past 35 kyr (Figure 8d), which occurred in at least two events, yielding a displacement rate of ~0.3 mm/yr. The two west dipping faults of Skull Valley have 20 ka

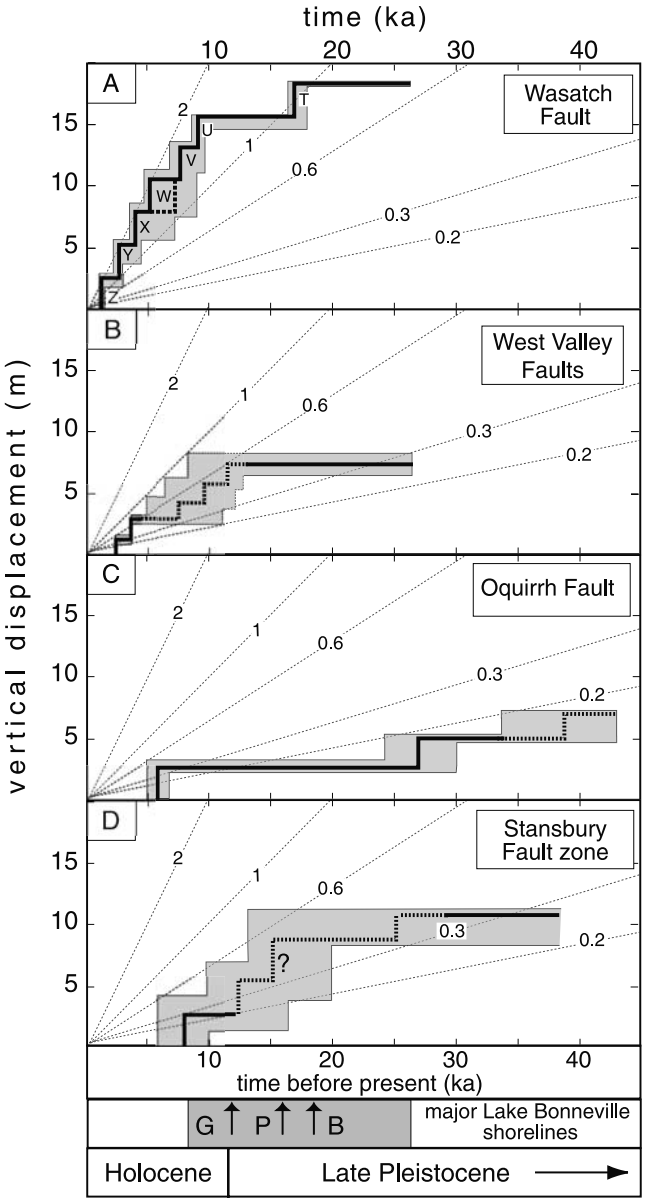

Figure 8. Holocene/Latest Pleistocene vertical displacement history of the (a) Wasatch, (b) West Valley, (c) Oquirrh, and (d) Stansbury faults, based on published paleoseismic data: Wasatch [*McCalpin and Nelson*, 2000; *Black et al.*, 1996]; West Valley [*Keaton et al.*, 1987]; Oquirrh [*Olig et al.*, 1994, 1996; *Handwerger et al.*, 1999]; Stansbury [*Hanson*, 1999; *Helm*, 1995]. The gray boxes indicate uncertainties in age or displacement discussed in text. Black arrows indicate the approximate age of shorelines associated with Lake Bonneville: G, Gilbert; P, Provo; and B, Bonneville highstand shorelines. These shoreline ages are given in calendar years based on work by *Oviatt et al.* [1992]. See color version of this figure in the HTML.

displacement rates of 0.2 and <0.1 mm/yr, respectively [*Hanson*, 1999].

4.2. Hundred-Thousand-Year Timescale (Mid-Pleistocene)

[25] Holocene and latest Pleistocene deposits, mostly related to Lake Bonneville, blanket most low-relief areas along the central Wasatch front, the northern Oquirrh Mountains, and the Stansbury Mountains (Figure 6). Pre-Bonneville (>26 ka) displacement histories in this region are therefore constrained only where Pleistocene deposits are exposed at elevations higher than Lake Bonneville shorelines and in a few localities where younger deposits have been eroded away or quarried. Because of this mode of preservation, many surfaces cut by a fault are exposed in the upthrown footwall block, but offset counterparts in the hanging wall are often concealed [e.g., *Machette*, 1981].

[26] Since ~200 ka, two major pre-Bonneville lake highstands are preserved in the Wasatch region, the older known as the Little Valley and the younger known as the Cutler Dam (Figure 7) [*Scott et al.*, 1983; *Oviatt and McCoy*, 1988]. Little Valley deposition probably ended at the end of marine oxygen isotope stage 6 (~130 ka; Figure 7), which corresponds to the beginning of the last major interglacial cycle (stage 5), implied by an estimate of the age of the overlying Promontory geosol of >100 ka [*Scott et al.*, 1983]. Near the northernmost trace of the Wasatch fault, north of Brigham City, deposits of the Cutler Dam cycle unconformably overlie the Promontory geosol [*Oviatt and McCoy*, 1988] and are in turn overlain by the Fielding geosol, which predates the <26 ka Lake Bonneville sediments. Therefore the Cutler Dam cycle probably correlates with the stage 4 glacial (Figure 7), implying an age of 60 ± 20 ka [*Scott et al.*, 1983; *Keaton et al.*, 1987]. These ages are minima, because they assign the Little Valley and the Cutler Dam cycles to the two most recent pre-Bonneville glaciations in the marine record. Therefore displacement rates derived from offsets of these features are maxima.

[27] At Dry Creek, just south of the mouth of Little Cottonwood Canyon, deposits correlated with the Little Valley highstand interfinger with glacial outwash deposits [*Madsen and Currey*, 1979; *Scott et al.*, 1983]. These glacial deposits are assigned to the Bull Lake glaciation, named after type deposits along the northeast flank of the Wind River Range, Wyoming, and are known throughout the Rocky Mountain and Great Basin regions (Figure 7) [*Blackwelder*, 1915; *Scott et al.*, 1983; *Richmond*, 1986]. Cosmogenic dating of the type Bull Lake moraines (IX to XIII of *Chadwick et al.* [1997]) yielded ages of 95 to 130 ka. Apparent low erosion rates of these moraines indicate the true ages are at or near the maximum of this range, implying development at or near the end of marine isotope stage 6 at ~130 ka [*Phillips et al.*, 1997]. The youngest Bull Lake moraines (XIV and XV of *Chadwick et al.* [1997]) could be as young as ~110 ka and therefore correlate with marine isotope stage 5d (Figure 7), but the cosmogenic ages are inconsistent with the correlation of any Bull Lake moraines with post-5d glacial epochs [*Phillips et al.*, 1997].

[28] Aggradation of alluvial fans in the arid southwest generally occurs during the transition from glacial to interglacial conditions [*Bull*, 1991]. Relative ages of alluvial fans are assigned based on the development of their topsoils, the degree of fan dissection, and their height above active fans [e.g., *Machette*, 1981; *Dohrenwend et al.*, 1996]. More robust ages are based on correlation of their topsoils with regional geosols that have well-defined stratigraphic positions between lacustrine or glacial deposits, such as the Promontory and Fielding geosols (Figure 7) [e.g., *Scott et al.*, 1983]. The oldest alluvial fans exposed along the Wasatch fault are

estimated to be 200 ka (pre-Little Valley interglacial, isotope stage 7) to 600 ka [*Izett and Wilcox*, 1982; *Machette et al.*, 1992b], and intermediate age fan surfaces are estimated to be 70–130 ka [*Machette*, 1981; *Mattson and Bruhn*, 2001]. The youngest alluvial fans postdate latest Pleistocene Lake Bonneville deposits (Figure 7). Although few absolute ages exist on mid to late Pleistocene deposits in the Wasatch region, relative age control may be used to limit displacement rates.

4.2.1. Wasatch Fault Zone

[29] Offset across the Wasatch fault in the past 150–250 kyr is constrained at several localities along the Wasatch front. In the vicinity of Big Cottonwood Canyon of the Salt Lake segment, lacustrine deposits of the Little Valley cycle are offset ~30 m (Figure 6) [*Scott et al.*, 1983]. The Dry Creek glacial deposits (~130 ka assuming correlation with type Bull Lake) are exposed on both sides of the fault just south of the mouth of Little Cottonwood Canyon [*Madsen and Currey*, 1979]. The moraine crest is only preserved in the footwall, so the difference in elevation between the crest projected across the fault and equivalent glacial deposits in the hanging wall of 70 ± 10 m provides an upper bound for vertical displacement [*Madsen and Currey*, 1979; D. Currey personal communication, 2001]. Along the Nephi, Brigham, and Provo segments older alluvial fan surfaces appear to be offset 25 to 35 m [*Machette*, 1981; *Machette et al.*, 1992b]. On the basis of the greater maturity of topsoils developed on these fans relative to the Promontory geosol, their age is estimated at ~250 ka (at the end of isotope stage 8, Figure 7 [*Machette*, 1981]). The fastest vertical displacement rate permitted by any of these offsets is 0.7 mm/yr, derived by considering the Dry Creek glacial deposits to be as young as the youngest Bull Lake moraines (~110 ka) and using the maximum possible offset (80 m). However, Little Valley lake deposits (of the same age) are only offset ~30 m in a nearby area, so this estimate may be a factor of two or more too high. Assuming the age and displacement estimates of the older alluvial fan surfaces are correct, the average displacement rate since ~250 ka is only 0.1 to 0.3 mm/yr (Figure 9a) [*Machette*, 1981; *Machette et al.*, 1992a, 1992b].

4.2.2. West Valley Fault Zone

[30] A detailed Pleistocene displacement record exists for the West Valley fault zone based on offset lacustrine deposits and soil horizons exposed in trenches and drill cores [*Keaton et al.*, 1987, Figure 5]. Lacustrine deposits of the Cutler Dam Lake cycle (60 ± 20 ka) are offset by 14 ± 1 m, whereas Little Valley Lake deposits (~130 ka) are offset by 18 ± 1 m. These data suggest vertical displacement rates of <0.1 mm/yr between 130 and 60 ka and 0.1 to 0.2 mm/yr between 60 and 20 ka (Figure 9b) [*Keaton et al.*, 1987].

4.2.3. Oquirrh Fault Zone

[31] Along the southern Oquirrh fault zone, the fault trace is above Bonneville shorelines, so that interactions between the fault and mid-Pleistocene alluvial fans are not obscured (Figure 6) [e.g., *Lund*, 1996]. The oldest alluvial surface is offset by up to 25 m but has not been dated. An alluvial surface dated cosmogenically at 75 ± 5 ka is offset ~6 m, yielding an average vertical displacement rate of 0.12 ± 0.02 mm/yr (Figure 9c) [*Mattson and Bruhn*, 2001]. Along the northern Oquirrh fault zone, the most recent fault trace occurs either in pre-Quaternary bedrock or latest Pleistocene deposits, and therefore does not allow an estimate of a 100-kyr displacement rate.

4.2.4. Stansbury Fault Zone

[32] Similar to the Oquirrh fault zone, the northern portion of the Stansbury fault trace is either in bedrock or covered by young lacustrine and alluvial deposits that do not allow an estimate of a 100-kyr displacement rate (Figure 6). The southern portion of the main Stansbury fault trace offsets inactive alluvial fan deposits up to 25 m, but the age of these deposits is poorly constrained. In Skull Valley, buried >130 ka alluvial fans are offset 30–50 m based on borehole data [*Hanson*, 1999], suggesting a maximum vertical displacement rate since ~130 ka of 0.4 mm/yr (Figure 9d). The actual rate may be considerably lower, because the maximum age of the offset deposits is poorly constrained. On the other hand, this estimate does not include some 25 m of displacement of old fan surfaces documented to the east on the range-bounding Stansbury fault zone. On the basis of seismic reflection data and shallow boreholes for the East fault in Skull Valley, *Hanson* [1999] estimates a 9-m cumulative offset of a soil horizon across several fault splays. She interpret the horizon as the Promontory geosol unconformably overlain by Lake Bonneville deposits and, on the basis of soil maturity, estimate the age of the surface <60 ka (Figure 9d), suggesting an average vertical displacement rate since then of at least 0.17 mm/yr [*Hanson*, 1999].

4.3. Million-Year Timescale (Cenozoic)

[33] Long-term exhumation rates may be derived from offsets of Tertiary volcanic units in the Wasatch, Oquirrh, and Stansbury ranges and from thermochronologic data from footwall crystalline rocks in the Wasatch Range.

4.3.1. Wasatch Fault Zone

[34] Wasatch fault initiation may have occurred as early as 17 Ma, exhuming exposed portions of the footwall from depths of >11 km [*Parry and Bruhn*, 1986, 1987], at an average rate of 0.5 to 0.7 mm/yr (Appendix A). Although a constant unroofing rate cannot be ruled out, apparent slowing of exhumation rate with time is suggested by cooling history data. These data appear best explained by unroofing rates of ≥1 mm/yr in middle and late Miocene time, slowing to <0.5 mm/yr in Plio-Quaternary time (Figure 10). If correct, these histories imply >80% of footwall unroofing occurred in Miocene time (Figure 10 and Appendix A). Average Plio-Quaternary unroofing rates of >0.8 mm/yr are incompatible with the thermal history of the footwall (Appendix A).

4.3.2. Oquirrh and Stansbury Fault Zones

[35] The timing of fault initiation is not known for the Oquirrh and Stansbury faults, but extension in this region is thought to have started at 10–14 Ma [*Bryant et al.*, 1990]. Long-term displacement estimates for the Oquirrh fault zone to range from a minimum of 3 km vertical, based on displaced Paleozoic strata, to a maximum estimate of ~10 km horizontal, based on the extent of the preserved preextensional surface on the eastside of the range [*Helm*, 1995]. These estimates imply an average long-term vertical displacement rate of 0.2–0.4 mm/yr. Long-term displacement rates for the Stansbury fault are at least 0.1–0.3 mm/yr based on a 3 km offset of the ~11 Ma Salt Lake Formation [*Helm*, 1995].

5. Discussion

[36] In interpreting these data we first compare vertical rates at different timescales derived from geological infor-

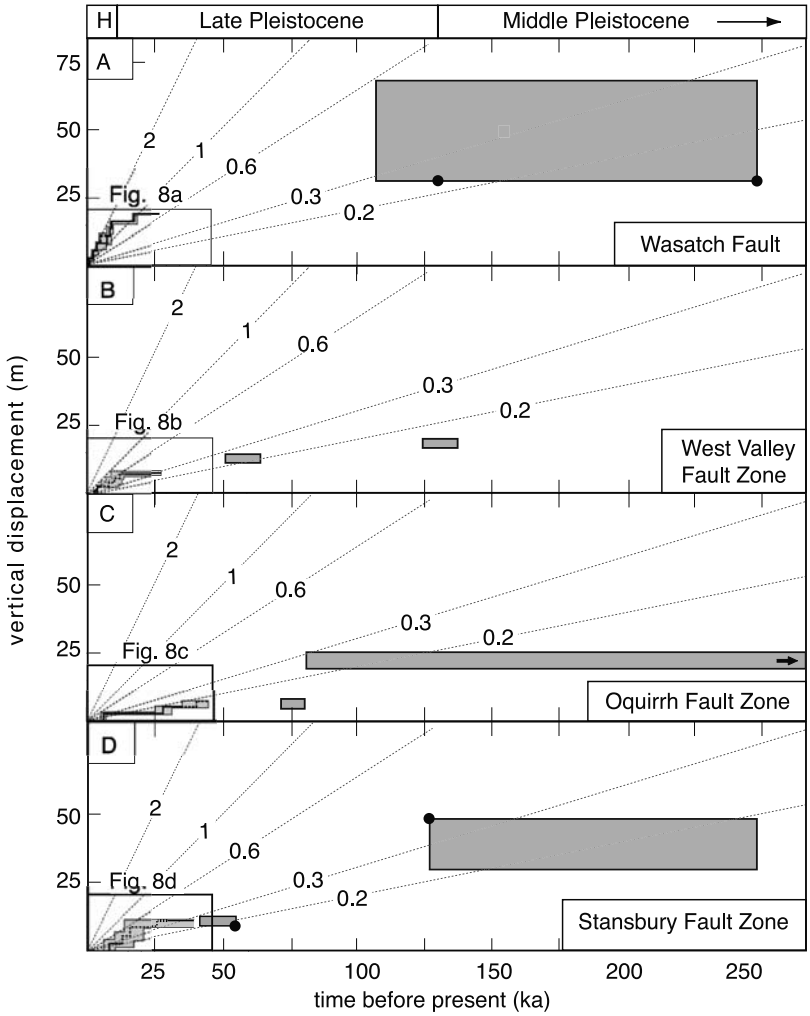

Figure 9. Compilation diagrams showing the mid-Pleistocene vertical displacement of the (a) Wasatch, (b) West Valley, (c) Oquirrh, and (d) Stansbury faults, based on offset geomorphic features discussed in text. Quantitative age control for offset alluvial fans is only available for one alluvial fan for the Oquirrh fault [*Mattson and Bruhn*, 2001]. Wasatch [*Machette et al.*, 1992b; *Machette*, 1981]; West Valley [*Keaton et al.*, 1987]; Oquirrh [*Olig et al.*, 1994, 1996; *Mattson and Bruhn*, 2001]; Stansbury [*Hanson*, 1999; *Helm*, 1995]. Black dots refer to displacement rates discussed in the text. See color version of this figure in the HTML.

mation, which generally reflect strain release. We then compare these rates with horizontal geodetic rates, which are the only proxy for strain accumulation, giving due consideration to the uncertainty in the average dip of the fault zones.

5.1. Comparison of Vertical Geologic Displacement Rates on the Wasatch Fault

[37] On the basis of the data summarized above, there appear to be significant variations in vertical motion on the Wasatch fault at different observed timescales. The average vertical exhumation rate since mid-Miocene time of 0.5–0.7 mm/yr is about twice the rate of 0.3 mm/yr averaged over the last 130–250 kyr. However, if the exhumation rate has slowed to <0.5 mm/yr in Plio-Quaternary time, then estimates for the 100-kyr timescale and the 1-Myr timescale would be in reasonable agreement. A slower Pliocene to recent extension rate in the Wasatch region is consistent with the generally lower extension rates throughout the northern Basin and Range province at this time [e.g., *Zoback et al.*, 1981; *Wernicke and Snow*, 1998; *Stockli*, 2000]. Regardless of whether these rates precisely agree, the post-6 ka rate of 1.7 ± 0.5 mm/yr is significantly higher than all of these estimates, except perhaps the highest estimates for the Miocene.

[38] Even though the late Miocene (5–10 Ma) and Holocene (0–10 ka) rates may agree, there is little reason to expect agreement given the much lower estimates for the Plio-Quaternary (0–5 Ma) and late Pleistocene (11–130 ka) timescales. This accords with the notion that changes in displacement rates at the million year timescale are controlled by changes in plate boundary forces or intraplate buoyancy, which are mainly sensitive to changes in relative plate motion and finite strains of continental lithosphere, respectively [e.g., *Atwater and Stock*, 1998; *Wernicke and Snow*, 1998; *Sonder and Jones*, 1999; *Flesch et al.*, 2000]. If these changes are insignificant on timescales of <1 Myr, agreement between the Plio-Quaternary (5 Ma to present)

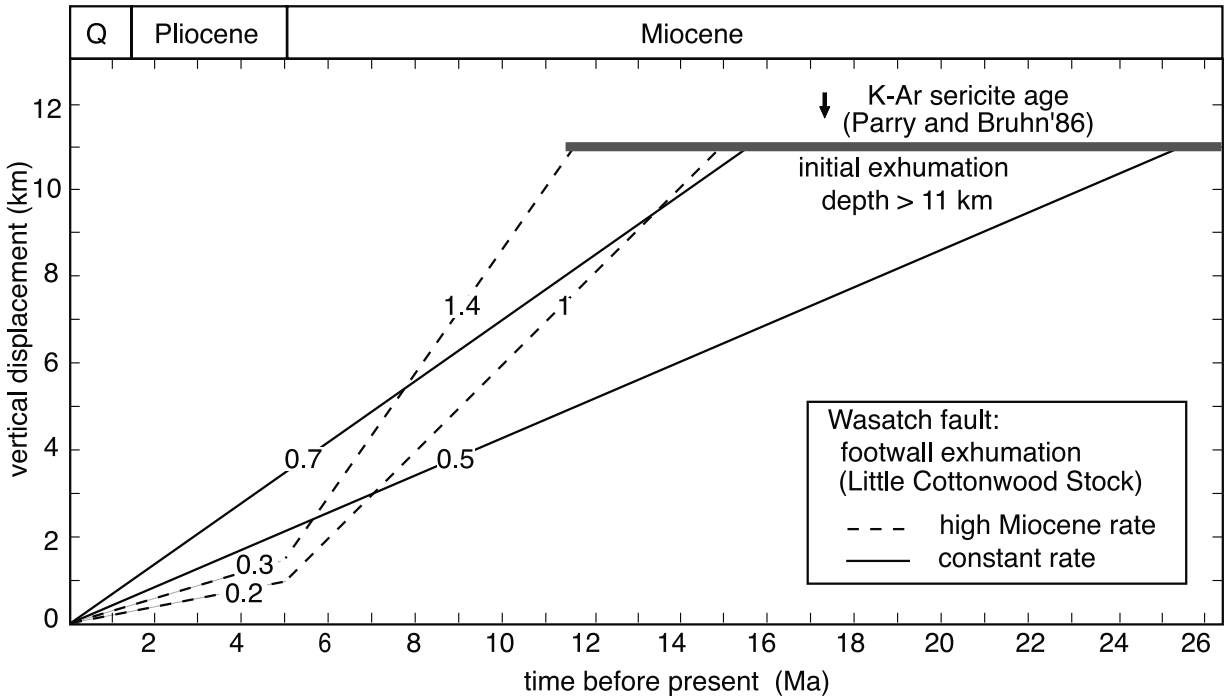

Figure 10. Summary of the million-year-scale vertical displacement history of the Wasatch fault discussed in Appendix A. Published thermochronologic and thermobarometric data are from the Little Cottonwood Stock along the Salt Lake segment of the Wasatch fault (Figure 4). Q, Quaternary. See color version of this figure in the HTML.

and late Quaternary (130 ka to present) rates would be expected. For the same reason, the large difference between the Holocene and late Quaternary rates would not be controlled by these processes, but rather more subtle factors such as the brittle rheology of fault zones, interactions between faults driven by coseismic changes in the regional stress field, stress diffusion effects, and other processes that may lead to clustered strain release.

[39] As discussed in section 1, in evaluating the relationship between strain accumulation and strain release it is critical to know whether measured strain is accumulating during or between clusters. In the case of the Salt Lake and other segments of the Wasatch fault, the time elapsed since the most recent event is of the same order as the Holocene recurrence interval (Figure 8a), implying that contemporary strain is accumulating during a cluster.

[40] Whether the contrast between the Holocene and latest Pleistocene is typical of the Wasatch fault, or of fault zones in general is an open question, because only one cluster is observed. On one hand, clustering may simply be the result of a random process where the variance of the earthquake repeat time is a large fraction of the average repeat time. On the other, if the pattern over the last 26 kyr is representative, there may be a bimodal distribution of repeat times. For the Salt Lake segment, the Holocene yields a minimum of ~14 m of displacement. If the simple bimodal distribution model is correct, it would require no more than three to four clusters since ~150 ka to account for the estimated displacement since then of ~30 to 70 m. The time-displacement record prior to 20 ka is not known in enough detail, however, to document any previous clusters.

[41] As to whether the Holocene cluster on the Wasatch fault bears some relation to the behavior on neighboring faults, we note that the Holocene displacement rates on the Oquirrh and Stansbury faults are much lower, indicating that clustered strain release during the Holocene was concentrated on the Wasatch (Figures 8 and 9). In contrast to the Wasatch, the Oquirrh and Stansbury Holocene displacement rates are not significantly different from their late Pleistocene rates.

5.2. Regional Context of the Holocene Cluster on the Wasatch Fault

[42] To determine the cumulative displacement history across the Wasatch, Oquirrh, and Stansbury faults on the Holocene and Pleistocene timescale, we added the individual displacement histories of the three west dipping normal faults across the transect and the east dipping West Valley faults (Figure 11). The cumulative vertical displacement rate is 2 to 4 mm/yr since 8 ka, but only 1 mm/yr between 8 and ~20 ka. Therefore, although adding the displacements of all the faults yields a somewhat more homogeneous strain release pattern, it does not appear to be uniform since 20 ka.

[43] The longer term vertical displacement rate across the transect was determined by adding the late Pleistocene (<130 ka) data for each fault. Because the Oquirrh fault is not observed to offset a 130 ka datum, we projected the displacement rate determined by the offset 70 ka alluvial fan back to 130 ka. The resulting vertical displacement rate across the transect is <1.2 mm/yr (Figure 11b), which is at best half the Holocene rate, but in agreement with the rate between 8 and 20 ka.

[44] The Holocene vertical displacement rate on the Wasatch fault thus accounts for most or all of the anomalous strain release in the region. The Holocene Wasatch rate also substantially exceeds those of most other normal faults

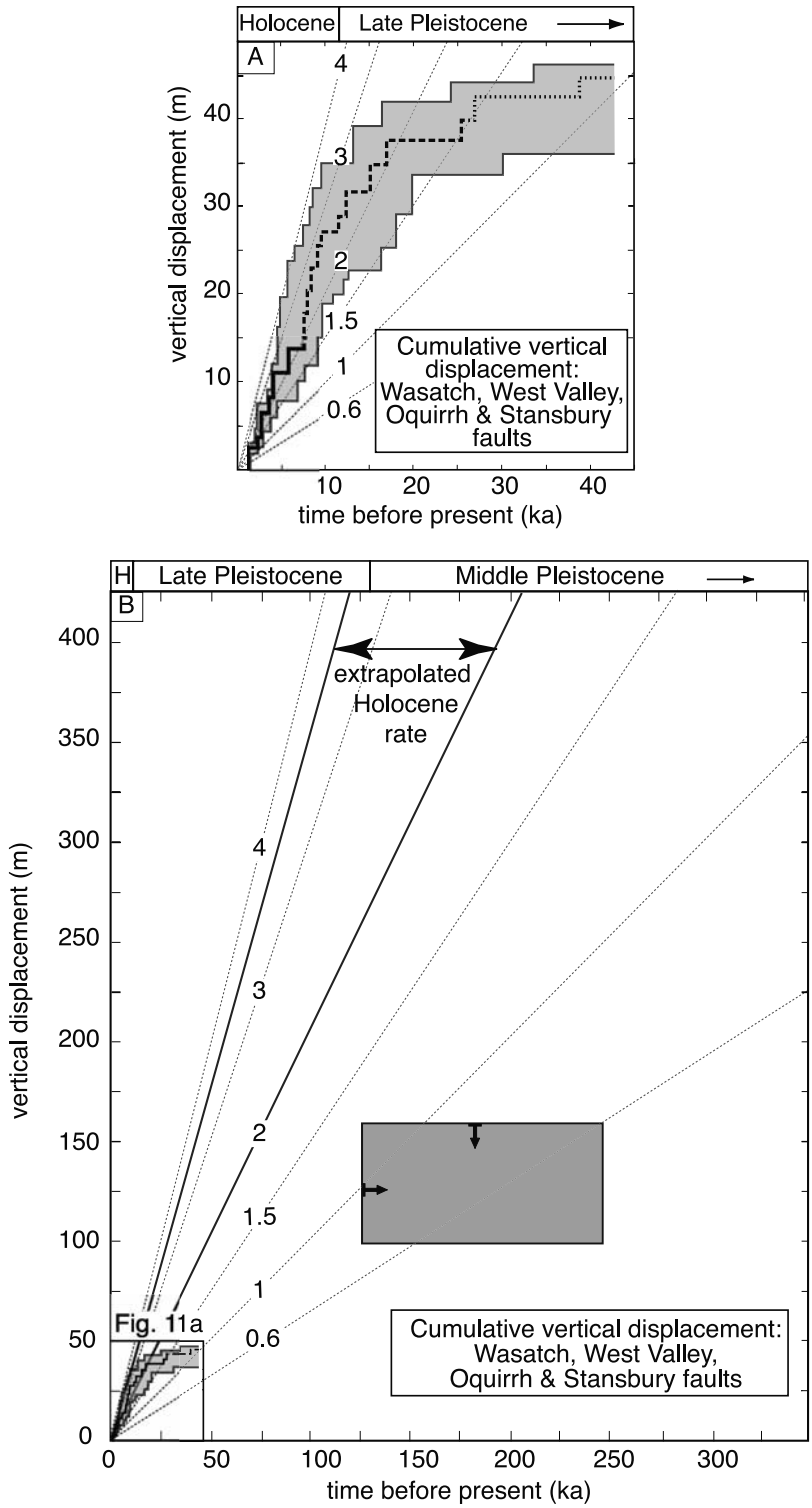

Figure 11. Cumulative vertical geologic displacement data based on data shown in Figures 8 and 9 for the Wasatch, West Valley, Oquirrh, and Stansbury faults: (a) latest Pleistocene and Holocene; (b) mid to late Pleistocene. The size of the gray shaded areas in both Figures 11a and 11b indicates the permissible range of slip rates based on published data. The arrows in Figure 11b indicate minimum constraints on the age and maximum constraints on the displacement. See color version of this figure in the HTML.

across the Basin and Range province [cf. *Caskey et al.*, 1996; *Bell et al.*, 1999; *Dohrenwend et al.*, 1996; *DePolo and Anderson*, 2000], which generally agree with presently available Pleistocene rates, apparently including those of the Wasatch itself, of approximately 0.2 to 0.4 mm/yr per fault [e.g., *Niemi et al.*, 2003].

[45] These comparisons collectively suggest that the Holocene cluster on the Wasatch fault is rather intense, and that the average recurrence time during this cluster is a small fraction of the length of the longest observed interseismic intervals (Figure 8). As mentioned above, comparison of the late Pleistocene and Holocene rates on the Wasatch indicates that no more than three to four clusters of the magnitude observed during the Holocene could have occurred since 130 ka, implying quiescent intervals of order of 30 to 40 kyr, assuming a bimodal distribution of repeat times.

5.3. Basis for Comparison of Geologic Vertical Fault Displacement Rates With Horizontal Geodetic Rates

[46] If, as appears to be the case for well-studied normal fault earthquakes, vertical displacement near the surface represents the vertical displacement averaged over the whole fault [*Niemi et al.*, 2003], vertical rates can be converted to horizontal rates by simple trigonometry, $h = v/\tan(d)$, where h and v are the horizontal and vertical displacement component, respectively, and d is the fault dip angle. For this model, if the faults dip $\sim 30^\circ$, then the horizontal displacement rates are $\sim$70% higher than the vertical rates (Figure 12a). For faults dipping 45° the implied horizontal rates would of course be the same as the vertical rates (Figure 12b), and for faults dipping 60° the horizontal rates would be $\sim$40% lower than the vertical rates (Figures 12b and 12c). Although dips of normal faults may rapidly decrease in some instances [e.g., *Gans and Bohrson*, 1998], major range-bounding faults have probably not tilted significantly in the last few hundred thousand years, and therefore we neglect any potential changes in fault dip in comparing contemporary, Holocene, and late Pleistocene displacement rates.

5.4. Comparison of Geologic Vertical Fault Displacement Rates With Horizontal Geodetic Rates

[47] With the above caveats in mind, it is noteworthy that (1) the horizontal rate across baseline HEBE-CEDA of 2.7 ± 0.2 mm/yr is consistent with the Holocene cumulative vertical rate across the region of 1.9–3.5 mm/yr (Figure 11 and Table 3) and (2) the horizontal rate across HEBE-COON of 1.9 ± 0.2 mm/yr agrees well with the Holocene vertical displacement rate across the Salt Lake segment of the Wasatch fault of 1.7 ± 0.5 mm/yr (Figure 12a). Compared with the longer timescale, however, the regional geodetic rate is about twice the maximum late Pleistocene rate of 1.3 mm/yr, and the HEBE-COON baseline is $\sim$3 times the maximum late Pleistocene rate for the Wasatch fault of 0.6 mm/yr (Figures 12a and 12b). Given the agreement of geodetic rates with the Holocene rates and the lack of agreement with the late Pleistocene rates, the most parsimonious interpretation is that strain accumulation and Holocene strain release are the same, and are therefore covariant on the 10-kyr timescale. If so, then Reid-type models (Figures 1a–1c) would be appropriate (Figure 12a). If not, then what we will refer to as Wallace-type behavior (Figure 1d) would apply.

[48] Thus the key question becomes whether this straightforward comparison may be compromised by potentially important uncertainties, including (1) the effective dips of the faults through the crust, (2) the contribution of transients such as stress diffusion to strain accumulation, and (3) the physical plausibility of marked variations in strain accumulation on the 10-kyr timescale. For example, if effective fault dips are near 30° across the transect, then the regional Holocene and Pleistocene horizontal rates would be $\sim$3.3–6.1 mm/yr and $\sim$0.7–2.3 mm/yr, respectively, and the Wasatch rates would be $\sim$2.9 and $\sim$0.2 to 1.0 mm/yr, respectively (Table 3). In this case, the geodetic rates would agree with the late Pleistocene rates, and imply Holocene strain release rates well in excess of geodetic rates (Figure 12b). Alternatively, if faults are as steep as 60°, then all strain release rates would be substantially lower than the geodetic rates (Table 3). In the absence of other considerations, then one may insist on either (1) steep (60°) normal faults or (2) Reid- or Wallace-type behavior, but not both. On the other hand, if the low dips of normal faults through the seismogenic crust observed in central Utah apply, Wallace-type behavior is implied.

[49] For slowly straining regions, such as the Basin and Range, a significant portion of the measured geodetic velocity field may be the result of transient strain that occurs in response to stress diffusion following earthquakes [*Elsasser*, 1969; *Foulger et al.*, 1992; *Hager et al.*, 1999; *Savage*, 2000; *Wernicke et al.*, 2000]. According to one simple model for a large Basin and Range earthquake with a relaxation time of $\sim$100 years, velocity anomalies of several millimeters per year within 60–80 km of a ruptured fault might be expected within the first two centuries after an event, and anomalies of order of a few tenths of millimeters per year within 200 km of the fault may persist through the first millennium [*Wernicke et al.*, 2000, Figure 5]. To the extent that relaxation times are much longer (e.g., 1000 years), much or all of geodetic signal may be a complex sum of effects from all Holocene earthquakes in the region.

[50] As described earlier, the last earthquake on the Salt Lake segment of the Wasatch fault occurred at $\sim$1.3 ka [*Black et al.*, 1996; *McCalpin and Nelson*, 2000], and the most recent event on the Wasatch fault occurred at $\sim$0.6 ka on the Nephi segment [*Schwartz et al.*, 1983; *Machette et al.*, 1992b], which is $\sim$100 km south of our geodetic transect. The most recent events on the Oquirrh and Stansbury faults occurred prior to 5 ka (Figure 8). Therefore the extant record of exposed fault segments suggests that viscoelastic contamination of the secular strain field is minor, unless relaxation times are significantly greater than $\sim$100 years.

[51] However, as mentioned earlier, the 90-km-long East Great Salt Lake fault ruptured $\sim$400 years ago in a $\sim M7$ event [*Dinter and Pechman*, 1999; D. Dinter and J. Pechman, personal communication, 2001], and has a southern terminus within 20 km of site COON (Figure 3). Given the proximity of such an event to the geodetic transect, and the recency and size of the event, stress diffusion effects related to this event could be an important component of the geodetic signal, even for relatively short relaxation times. Using the simple model mentioned above [*Wernicke et al.*, 2000, Figure 5c], an event 400 years ago would result in a velocity anomaly of 1 mm/yr within 100 km of the fault,

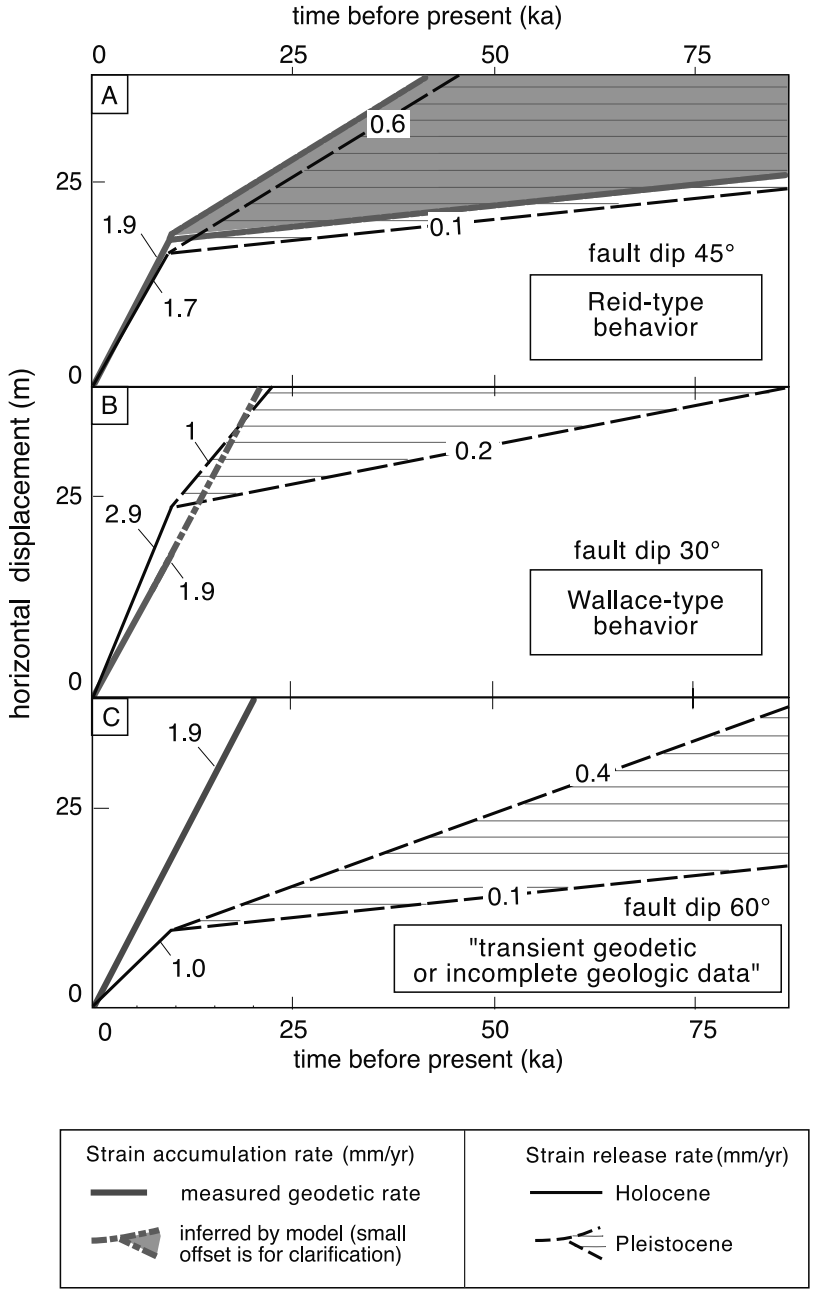

Figure 12. Comparison of geodetically measured horizontal strain rates with horizontal components of geologic displacement rates for the Wasatch fault. The vertical geological rates were converted to horizontal rates by assuming effective fault dips of (a) 45°, (b) 30°, and (c) 60°. The geodetically measured rate is strictly only valid for the measurement interval, 1996–2000, but has been plotted for comparison with the geologic rates. See color version of this figure in the HTML.

and strain rates near 20 nstrain/yr, accounting for most of the observed signal.

[52] It is noteworthy in this regard that the maximum strain rate in the geodetic transect is centered roughly on site COON, and not along the Wasatch fault zone, as might be expected on the basis of vertical displacement rates. Therefore the most recent event on the East Great Salt Lake fault may account not only for all of the regional strain rate above the Basin and Range average of 10 nstrain/yr near the fault, but also for the apparent retardation of strain just east of the Wasatch fault and between CEDA and GOSH, to levels well below the Basin and Range average [*Wernicke et al.*, 2000, Figure 5]. If this is correct, then strain accumulation across the transect would be more consistent with the Late Pleistocene rates (regardless of fault dip), and Wallace-type behavior would be strongly favored as an explanation of the Holocene cluster on the Wasatch fault.

[53] A final consideration is that if the faults do not have shallow dip, and the most recent event on the East Great Salt Lake fault zone is not significant, then Reid-type behavior, with strongly variable strain accumulation on the 10,000-year timescale, would most simply explain the

Table 3. Comparison of Geodetic (BARGEN) Rates With Geologic Rates Across the Wasatch Fault and the Transect Region

	Horizontal Geodetic Rate,[a,b] mm/yr (1996–2000)	Vertical Geologic Displacement Rates,[c,d] mm/yr				Horizontal Geologic Rate, mm/yr			
						Effective Fault Dip of 30°		Effective Fault Dip of 60°	
		Holocene (0–10 ka)	Pleistocene (0–130 ka)	Plio-Q (0–5 Ma)	Miocene (5–15 Ma)	Holocene	Pleistocene	Holocene	Pleistocene
Wasatch fault	1.9 ± 0.2	1.7 ± 0.5	0.1 − 0.6	0.2 − 0.7	0.5 − 1.4	2.9 ± 0.5	0.2 − 1.0	1.0 ± 0.5	0.1 − 0.4
Regional transect[e]	2.7 ± 0.2	1.9 − 3.5	0.4 − 1.3	0.4 − 1.2	n/a	3.3 − 6.1	0.7 − 2.3	1.1 − 2.0	0.2 − 0.8

[a]Horizontally measured geodetic rates for baseline HEBE-COON across the Wasatch fault, and HEBE-CEDA across the regional transect.
[b]Including the Wasatch, West Valley, Oquirrh, and Stansbury faults.
[c]For effective fault dips of 45°, the vertical rates reported in these columns equal to the horizontal displacement components.
[d]These rates are discussed in the text, and shown as displacement time plots in Figures 10 to 13.
[e]Measurements are reported at the 1σ uncertainty level.

comparisons of rates. On one hand, such behavior seems unlikely because it is difficult to envisage a physical mechanism that would vary the strain accumulation rates on individual faults on this timescale, given that local transient effects are presumed insignificant. On the other, if correct, a major process is at work governing fault system behavior that is only now coming to light.

[54] If strain accumulation in the eastern Basin and Range is relatively uniform, perturbed mainly by relatively brief postseismic relaxation [*Wernicke et al.*, 2000; *Niemi et al.*, 2003] and strain release is governed by Wallace-type behavior, then three dominant timescales of variation might be expected in the geodetic and geologic strain fields, at $\sim 10^7$, 10^4, and 10^2 years (Figure 13). The first is reflected in both strain accumulation and release (geodetic and geologic fields), and is measured using geological criteria ranging in age from 10^5 to 10^7 years (Figure 13a), with a displacement amplitude on the order of kilometers. A change in rate from 1.5 to 0.3 mm/yr (m_4 to m_1, Figure 13a) yields a variation in velocity of order 1 mm/yr with a period of order 10^7 years, presumably driven by large, slow variations in regional tectonic stress. The second timescale may be represented mainly in strain release behavior, with displacement amplitudes of order tens of meters and velocity amplitude of order mm/yr (m_2, Figure 13b). This model presumes quasiperiodic repetition of earthquake clusters every $\sim 10^4$ years, presumably caused by an interaction between brittle constitutive behavior and relatively small perturbations in stress (Figure 13b). At this timescale, only the geologic displacement field varies at the amplitude of tens of meters, with the geodetic field (assuming we could measure it) presumably having little commensurate variation. The third would reflect local transients (velocity m_3, Figure 13c), which would not be directly recorded in the geologic signal at the millennial timescale (velocity m_2, Figure 13b).

[55] The main implication of this hypothesis is that the short-timescale strain release history (m_2) will generally not agree with the geodetic rate (m_3) or the long-term strain accumulation rate (m_1). If so, agreement between the geodetic rate and Holocene strain release rate along the Wasatch fault zone would be a coincidence of strain release processes at the 10^4 year timescale and stress diffusion phenomena operative at the 10^2 year timescale.

6. Conclusions

[56] Despite the unusually complete temporal record for the Wasatch and related faults, uncertainties in subsurface fault geometry, the ages of late Quaternary deposits in the region, and the magnitude of postseismic transient effects on the geodetic signal, preclude distinguishing between "Reid-type" and "Wallace-type" models for earthquake recurrence (Figure 14). The data imply, however, that if "Reid-type" models are valid, a process or processes control significant variations in the strain accumulation rate of crustal fault zones at timescales of $\sim 10^4$ years. If no such process exists, then the data lean toward a "Wallace-type" model. Given the amplitudes of variation in displacement and velocity in the Wasatch region (Figure 14a), the amplitudes of periodic, geologically determined earth deformation would have maxima of kilometers at periods of 10^7 years and tens of meters near periods of 10^4 years (assuming periodic clusters), with velocity amplitudes of order 1 mm/yr at both periods (Figures 14b and 14c). In terms of strain accumulation (only measurable geodetically at short timescales), the amplitude spectrum would be similar at periods of 10^7 years, but instead of a peak at 10^4 years, would have maxima in displacement and velocity of order decimeters and millimeters per year, respectively, at a period of 10^2 years (Figure 14b). If correct, the latter hypothesis predicts that geodetic, paleoseismological, and geological estimates of fault slip rates will in general differ.

Appendix A: Exhumation History of the Wasatch Fault

[57] Reconstruction of the displacement history of the Wasatch fault on the million-year timescale is based on published thermochronologic and thermobarometric data on the Oligocene Little Cottonwood stock (Figure 4). As mentioned in the text, the net result of slip along the Wasatch fault zone was to exhume a >11-km-thick crustal section through thrust-faulted miogeoclinal sediments (country rock to the stock) unconformably overlain by Oligocene volcanics, now tilted eastward some 20°–30° (Figure 4) [*Parry and Bruhn*, 1987]. Compared with this exhumation, net subsidence of the hanging wall is minor (~1 km), and therefore footwall unroofing is a reasonable proxy for long-term net vertical tectonic displacement.

[58] At deepest structural levels along the west side of the range near the mouth of Little Cottonwood Canyon, fault rocks are developed at the expense of quartz monzonite of the stock (locality A in Figure 4). At shallowest structural levels along the east flank of the range, Tertiary volcanics dip 20°–35° eastward (Figure 4) [*Bryant*, 1990, 1992]. Although the pre-Tertiary strata are complexly deformed, they broadly

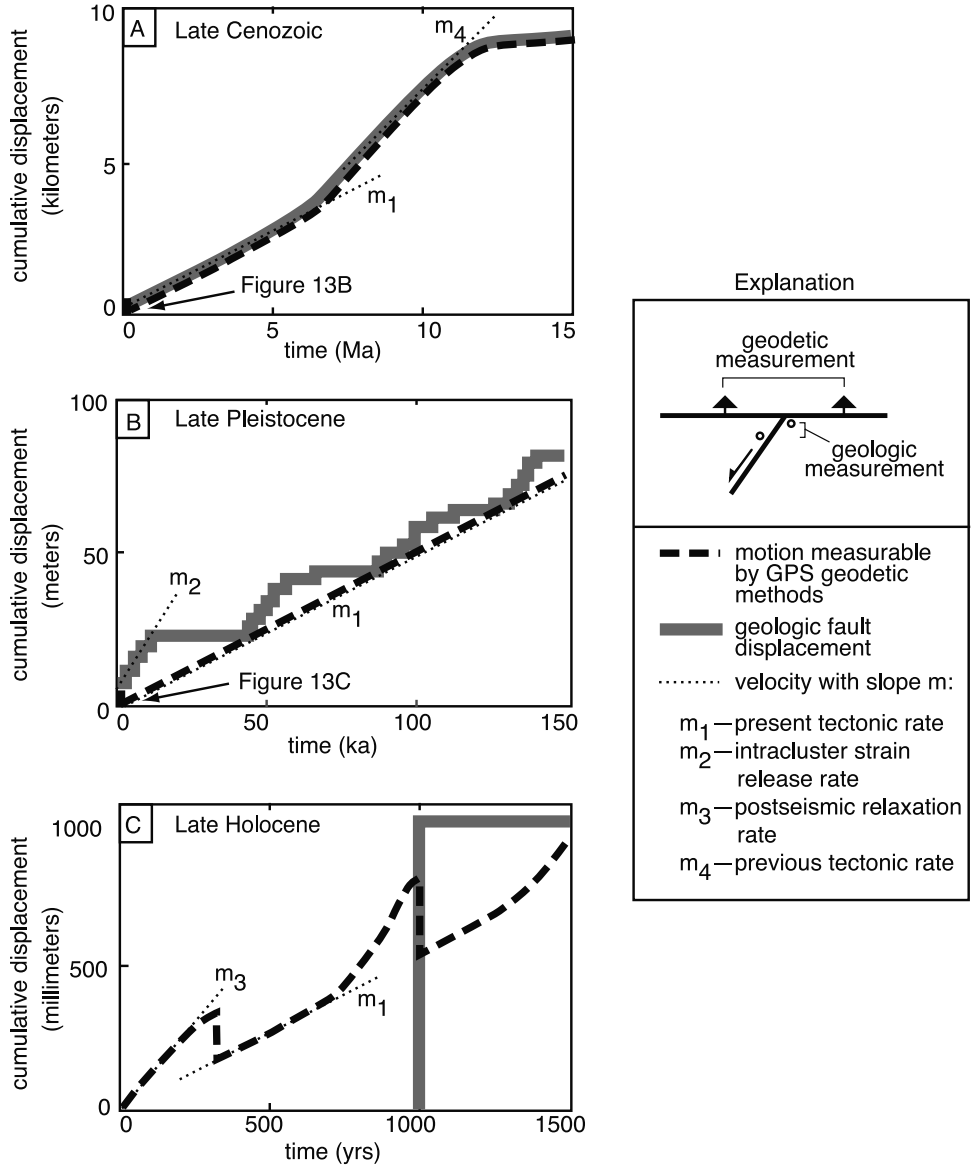

Figure 13. The significance of geologic and geodetic measurements for typical intracontinental faults on (a) the 10^6 year, (b) the 10^4 year, and (c) the 10^2 year timescales. The black dashed line represents relatively far-field geodetic motions partly affected by coseismic offsets and postseismic strain transients. See color version of this figure in the HTML.

define a thrust-faulted passive margin wedge also tilted ~25° to the east along the crest of a major pre-Tertiary antiform (Figure 4) [*Parry and Bruhn*, 1987]. Therefore, if the range is an east tilted section, the pretilt depth of locality A (Figure 6) would be ~10–15 km. Fluid inclusions from the fault rocks indicate an equilibration depth of >11 km and maximum temperatures of ~350°C [*Parry and Bruhn*, 1987; *John*, 1989], in accord with this expectation.

[59] The timing of exhumation is constrained mainly by published zircon and apatite fission track ages [*Kowallis et al.*, 1990]. Assuming present horizontal position between the Tertiary unconformity and locality A (Figure 4) varies linearly with paleodepth in the crustal section, and assuming a preunroofing geothermal gradient, we may estimate the positions of the apatite and zircon partial annealing zones within the section. On the basis of the work by *Bryant* [1990] and the assumption that the decollement surfaces in the thrust system were subhorizontal prior to tilt, we have assumed an average of 22° east tilt, and a preunroofing geothermal gradient of 30°C/km [*Parry and Bruhn*, 1986; *Ehlers and Chapman*, 1999]. Assuming temperatures of full annealing of 110°C for apatite and 230°C for zircon, the base of the partial annealing zone for apatite lay approximately halfway between the Tertiary unconformity and the Wasatch fault, and the base of the zircon partial annealing zone lay near the Wasatch fault prior to tilting and exhumation (Figure 4).

[60] Apatite fission track ages both near the Wasatch fault and ~8 km to the east at Lone Peak (locality B, Figure 4) yield ages of 5 to 11 Ma (Figure A1). Zircon fission track ages near the Wasatch fault are nearly concordant with the older apatite ages (~9 to 11 Ma), but at Lone Peak are much older, at ~20 Ma [*Kowallis et al.*, 1990]. Plotted as a

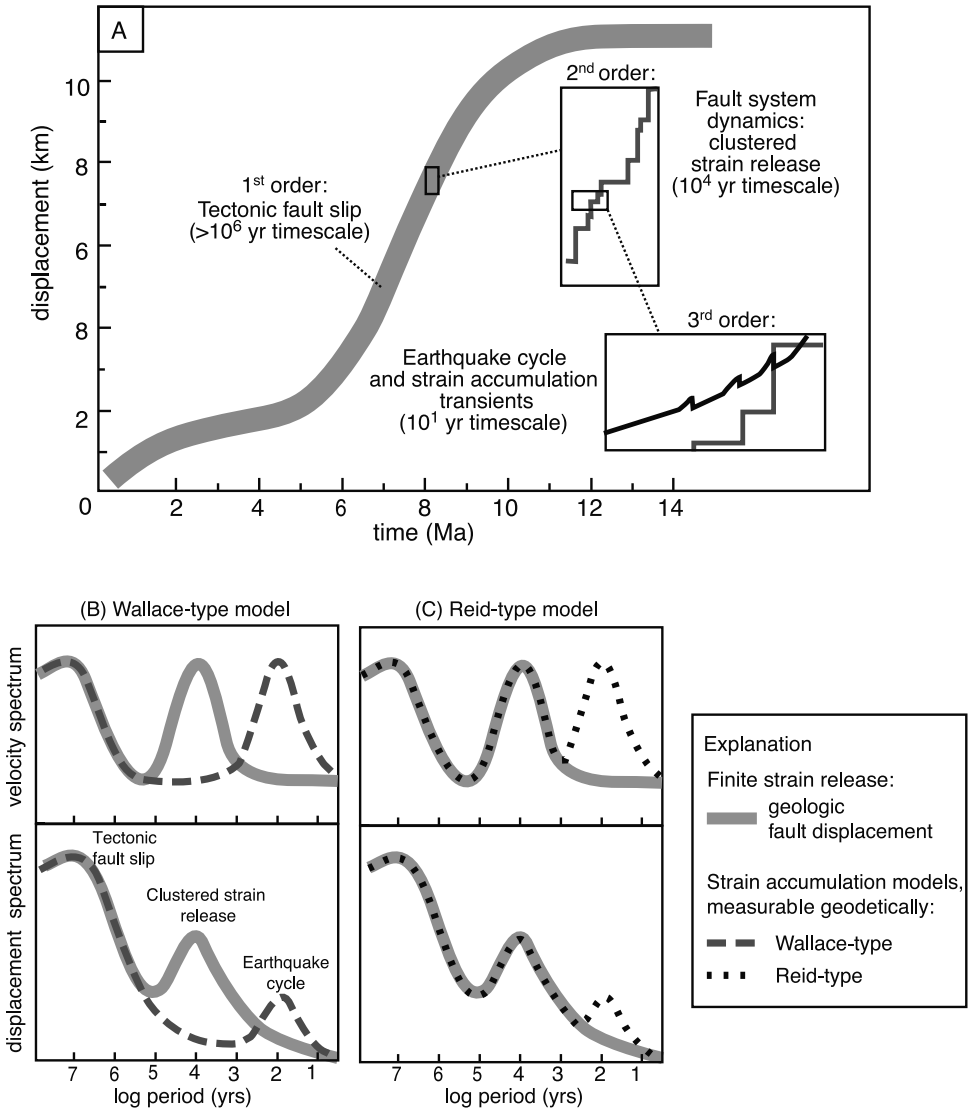

Figure 14. (a) Schematic diagram showing the superposition of tectonic, fault dynamic, and transient processes at three different amplitudes and periods. See Figure 13 for explanation of symbols. (b) Spectral character of the velocity and displacement fields for Earth deformation for "Wallace-type" deformation and (c) "Reid-type" deformation. See color version of this figure in the HTML.

function of inferred paleodepth below the basal Tertiary unconformity assuming tilt of 22°, the observed pattern is consistent with the base of the zircon PAZ at or near the western range front prior to unroofing, and with the base of the apatite PAZ somewhere to the east of the eastern samples (Figure 4). This pattern is corroborated by recent fission track and (U-Th)/He apatite ages (Figure A1) [*Armstrong et al.*, 2000]. Apatite fission track ages range from 15 to 30 Ma well to the east of Lone Peak, and from 4 to 10 Ma to the west, perhaps decreasing slightly with inferred paleodepth. (U-Th)/He apatite ages are ~5–6 Ma on Lone Peak younging with inferred paleodepth to values as low as 2 Ma at the range front.

[61] For the group of samples near the Wasatch front (locality A, Figure 4), the zircon and apatite fission track ages indicate cooling between ~10 and ~6 Ma, apparently quenching the extant fossil partial annealing zones in apatite and zircon. The difference of ~4 Myr in apatite and zircon fission track ages, assuming a 120°C difference in annealing temperatures, suggests cooling rates of ~30°C/Myr. A similar age difference between apatite fission track and (U-Th)/He ages, assuming a 40°C difference in closure temperatures, implies latest Miocene and Pliocene cooling rates of 10°C/Myr (Figure A1).

[62] Because the implied unroofing rates are in the mm/yr range, due consideration must be given to the interplay between advection and conduction in deriving the unroofing history [e.g., *Ruppel et al.*, 1988; *Moore and England*, 2001]. Where conduction dominates, time-temperature histories may be converted directly to unroofing rates if the geothermal gradient during unroofing is known. Thus, for the Wasatch cooling history profiles shown in Figure A2, ignoring advection would suggest unroofing rates of ~1 mm/yr from 10 to 6 Ma and rates of 0.3 mm/yr from 6 to 2 Ma. When advection becomes important, in general, the more rapid the unroofing rate, the greater the time lag

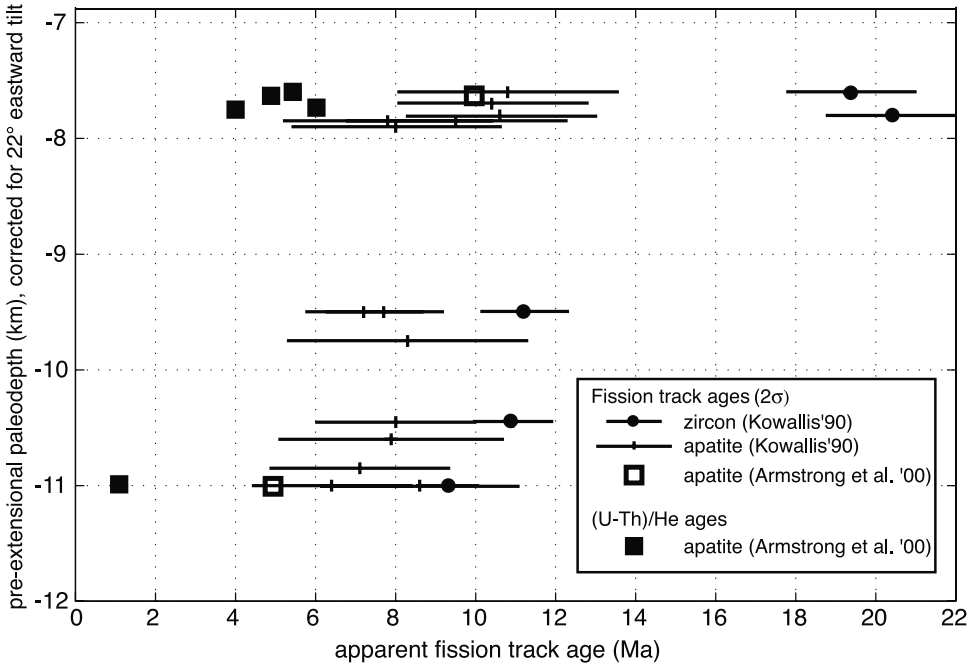

Figure A1. Age versus paleodepth plot of published apatite and zircon fission track, and apatite (U-Th)/He data for the Little Cottonwood Stock, Wasatch range [*Kowallis et al.*, 1990; *Armstrong et al.*, 2000]. The paleodepth has been corrected for a 22° east tilt of the range. See color version of this figure in the HTML.

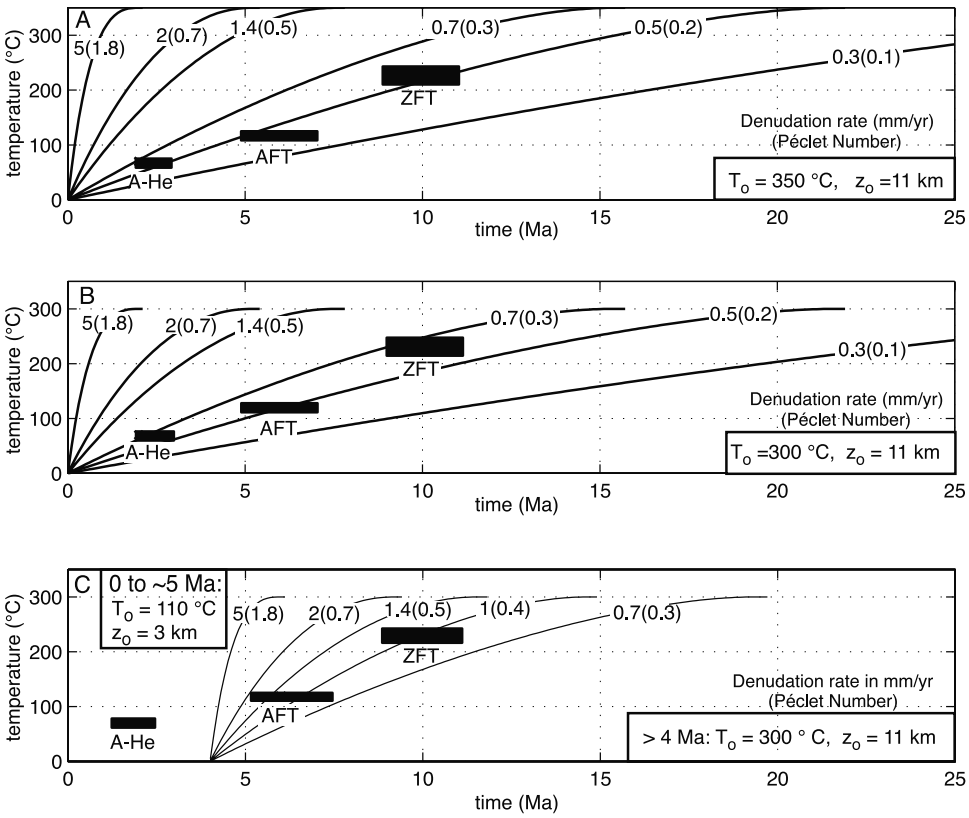

Figure A2. Cooling history of the Wasatch fault based on apatite fission track (AFT), zircon fission track (ZFT), and apatite (U-Th)/He (A-He) ages and thermal modeling based on *Moore and England* [2001]. T_0, initial temperature; z_0, initial depth. See color version of this figure in the HTML.

between the onset of unroofing and significant cooling, and the greater the apparent unroofing rate becomes by directly converting the cooling rate through the geothermal gradient [*Moore and England*, 2001].

[63] The simplest unroofing model would be one of constant unroofing rate. Using the parameterization of *Moore and England* [2001], it is difficult to fit a single unroofing rate to the Wasatch cooling curve, because the cooling curve suggests decreasing cooling rates with time, and all constant rate unroofing models, except those which neglect advection, predict increasing cooling with time (Figure A2). Nonetheless, given the uncertainties in isotopic ages and their closure temperatures, the cooling curves are consistent with constant unroofing rates of 0.5 to 0.7 mm/yr since 15 to 20 Ma, respectively, assuming a starting depth of 11 km. Models with constant unroofing rates of more than ~0.8 mm/yr do not fit the data.

[64] If the apparent decrease in cooling rate reflects decreasing unroofing rate with time, models more complicated than that of *Moore and England* [2001] would need to be evaluated. For example, if a change in unroofing rate occurred at ~4 Ma (just after annealing began in apatite but before He retention) the upper part of the cooling curve would be compatible with a model unroofing rate of ~1.0 to ~1.4 mm/yr beginning at 13 and 15 Ma, respectively (Figure A2c). However, rates this rapid early in the cooling history require rates of only 0.2 to 0.3 mm/yr after 4 Ma (Figure 12). Relatively low unroofing rates since ~4 Ma, in the absence of other considerations, would imply a low Peclet number and therefore allow estimation of unroofing rates through an assumed geotherm. For cooling rates of 10°C/Myr through a geothermal gradient of 30°C/km [*Ehlers and Chapman*, 1999], unroofing rates would be 0.3 mm/yr, in reasonable agreement with a two-stage model (Figure 10).

[65] A K-Ar age on sericite from sheared and altered quartz monzonite in the damage zone of the fault is 17.6 ± 0.7 Ma [*Parry and Bruhn*, 1986]. Although this age appears to be relatively old, compared with the apatite and zircon fission track data, a prediction of the unroofing models in Figure A2 is that cooling begins relatively slowly once unroofing begins. Further, it is possible that the earliest unroofing was relatively slow. In any event, this age is difficult to interpret in the absence of step-heating experiments that would reveal isotope correlation behavior and other standard criteria for evaluating argon ages.

[66] In summary, the cooling history data from deeply exhumed rocks near the trace of the Wasatch fault are compatible with a constant unroofing rate of ~0.5 to 0.7 mm/yr since middle Miocene time [e.g., *Kowallis et al.*, 1990]. However, the apparent slowing of cooling rate suggested by the (U-Th)/He data, if real, is most simply explained by relatively rapid unroofing of the footwall at ~1 mm/yr in middle and late Miocene time, slowing to an average rate of <0.5 mm/yr in Pliocene and Quaternary time. The data are incompatible with Plio-Quaternary rates in excess of ~0.8 mm/yr.

[67] **Acknowledgments.** This research was supported by National Science Foundation grants EAR-97-25766 and 99-03366 awarded to B. Wernicke and NASA grant NAG5-8226 and USGS 99HQGR0212 awarded to R. Bennett. We thank F. Albarede, W. Thatcher, S. Wesnousky and an anonymous reviewer for constructive comments that greatly improved the presentation. We thank J. Bartley, D. Currey, K. Haller, M. Machette, K. Hanson, E. Lips, A. Mattson, S. Olig, J. Pechman, M. Simons, and R. B. Smith for useful discussions on the geophysics and Quaternary history of the Wasatch region. Special thanks to D. Dinter and J. Pechmann for permission to discuss unpublished data on the seismic history of the East Great Salt Lake fault and to E. Lips for permission to discuss unpublished data on the late Quaternary history of the Little Cottonwood area.

References

Allmendinger, R. W., J. W. Sharp, D. Von Tish, L. Serpa, L. Brown, S. Kaufmann, J. Oliver, and R. B. Smith, Cenozoic and Mesozoic structure of the eastern Basin and Range Province, Utah, from COCORP seismic-reflection data, *Geology*, *11*, 532–536, 1983.

Armstrong, P. A., T. A. Ehlers, P. J. J. Kamp, K. A. Farley, D. S. Chapman, and Anonymous, Tracking changes in exhumation rates using low-temperature thermochronometry; an example from the Wasatch Mountains, Utah (USA), in *Fission Track 2000; 9th International Conference on Fission Track Dating and Thermochronology*, pp. 5–7, Geol. Soc. of Aust., Sydney, 2000.

Arnow, T., and R. E. Mattick, Thickness of valley fill in the Jordan Valley east of the Great Salt Lake, Utah Geological Survey research 1968, Chap. B, U.S. Geol. Surv., Reston, Va., 1968.

Atwater, T., and J. Stock, Pacific-North America plate tectonics of the Neogene of the southwestern United States; an update, *Int. Geol. Rev.*, *40*, 375–402, 1998.

Bell, J. W., C. M. dePolo, A. R. Ramelli, A. M. Sarna-Wojcicki, and C. E. Meyer, Surface faulting and paleoseismic history of the 1932 Cedar Mountain earthquake area, west-central Nevada, and implications for modern tectonics of the Walker Lane, *Geol. Soc. Am. Bull.*, *111*(6), 791–807, 1999.

Bennett, R. A., B. P. Wernicke, and J. L. Davis, Continuous GPS measurements of contemporary deformation across the northern Basin and Range, *Geophys. Res. Lett.*, *25*, 563–566, 1998.

Bennett, R. A., J. L. Davis, and B. P. Wernicke, Present-day pattern of Cordilleran deformation in the Western United States, *Geology*, *27*(4), 371–374, 1999.

Bennett, R. A., B. P. Wernicke, N. A. Niemi, A. M. Friedrich, and J. L. Davis, Contemporary strain rates in the northern Basin and Range province from GPS data, *Tectonics*, *22*(2), 1008, doi:10.1029/2001TC001355, 2003.

Black, B. D., W. R. Lund, D. P. Schwartz, H. E. Gill, and B. H. Mayes, Paleoseismic investigation on the Salt Lake City segment of the Wasatch fault zone at the South Fork Dry Creek and Dry Gulch sites, Salt Lake County, Utah, *Spec. Stud. 92*, 22 pp., Utah Geol. Surv., Salt Lake City, 1996.

Blackwelder, E., Cenozoic history of the mountains of central Wyoming, *J. Geol.*, *23*, 97–117, 1915.

Bruhn, R. L., P. R. Gibler, W. Houghton, and W. T. Parry, Structure of the Salt Lake Segment, Wasatch normal fault zone; implications for rupture propagation during normal faulting, in *Assessing Regional Earthquake Hazards and Risk Along the Wasatch Front, Utah*, edited by P. A. Gori and W. W. Hays, *U.S. Geol. Surv. Prof. Pap.*, *1500*, H1–H25, 1992.

Bryant, B., Geologic map of the Salt Lake City 30′ × 60′ quadrangle, north central Utah and Uinta County, Wyoming, *U.S. Geol. Surv. Misc. Invest. Ser. Map*, *I-1944*, scale 1:100,000, 1990.

Bryant, B. H., Geologic and structure maps of the Salt Lake City 1° × 2° quadrangle, Utah and Wyoming, *U.S. Geol. Surv. Misc. Invest. Ser. Map*, *I-1997*, scale 1:125,000, 1992.

Bryant, B., C. W. Naeser, R. F. Marvin, and H. H. Mehnert, Ages of late Paleogene and Neogene tuffs and the beginning of rapid regional extension, eastern boundary of the Basin and Range Province near Salt Lake City, Utah, in Upper Cretaceous and Paleogene sedimentary rocks and isotopic ages of Paleogene tuffs, Uinta Basin, Utah, *U.S. Geol. Surv. Bull.*, *1787*, K1–K12, 1990.

Bull, W. B., *Geomorphic Responses to Climatic Change*, 326 pp., Oxford Univ. Press, New York, 1991.

Bull, W. B., Correlation of fluvial aggradation events to times of global climate change, in *Quaternary Geochronology: Methods and Applications*, *Ref. Shelf*, vol. 4, edited by J. S. Noller, J. M. Sowers, and W. R. Lettis, pp. 456–464, AGU, Washington, D. C., 2000.

Caskey, S. J., S. G. Wesnousky, Z. Peizhen, and D. B. Slemmons, Surface faulting of the 1954 Fairview Peak (M_s 7.2) and Dixie Valley (M_s 6.8) earthquakes, central Nevada, *Bull. Seismol. Soc. Am.*, *86*(3), 761–787, 1996.

Chadwick, O. A., R. D. Hall, and F. M. Phillips, Chronology of Pleistocene glacial advances in the Central Rocky Mountains, *Geol. Soc. Am. Bull.*, *109*(11), 1443–1452, 1997.

Cook, K. L., J. W. Berg Jr., W. W. Johnson, and R. T. Novotny, Some Cenozoic structural basins in the Great Salt Lake area, Utah, indicated by regional gravity surveys, in *The Great Salt Lake*, *Guideb. Geol. Utah*, *20*, 57–75, 1966.

Crone, A. J., M. N. Machette, M. G. Bonilla, J. J. Lienkaemper, K. L. Pierce, W. E. Scott, and R. C. Bucknam, Surface faulting accompanying the Borah Peak earthquake and segmentation of the Lost River Fault, central Idaho, *Bull. Seismol. Soc. Am.*, *77*(3), 739–770, 1987.

Davis, J. L., R. A. Bennett, and B. P. Wernicke, Assessment of GPS velocity accuracy for the Basin and Range Geodetic Network (BARGEN), *Geophys. Res. Lett.*, *30*, 10.1029/2003GL016961, in press, 2003.

DeCelles, P. G., T. F. Lawton, and G. Mitra, Thrust timing, growth of structural culminations, and synorogenic sedimentation in the type Sevier orogenic belt, western United States, *Geology*, *23*(8), 699–702, 1995.

DePolo, C. M., and J. G. Anderson, Estimating the slip rates of normal faults in the Great Basin, USA, *Basin Res.*, *12*, 227–240, 2000.

Dimitru, T. A., Fission-track geochronology, in *Quaternary Geochronology: Methods and Applications*, *Ref. Shelf*, vol. 4, edited by J. S. Noller, J. M. Sowers, and W. R. Lettis, pp. 131–156, AGU, Washington, D. C., 2000.

Dinter, D. A., and J. C. Pechmann, Multiple Holocene earthquakes on the East Great Salt Lake fault, Utah: Evidence from High-resolution seismic reflection data, *Eos Trans. AGU*, *80*(46), Fall Meet. Suppl., F735, 1999.

Dohrenwend, J. C., B. A. Schell, C. M. Menges, and B. C. Moring, Reconnaissance photogeologic map of young (Quaternary and late Tertiary) faults in Nevada, in *An Analysis of Nevada's Metal-Bearing Mineral Resources*, edited by D. A. Singer, Plate 9-6, Nev. Bur. of Mines and Geol., Reno, 1996.

Doser, D. I., Extensional tectonics in northern Utah-southern Idaho, U.S.A., and the 1934 Hansel Valley sequence, *Phys. Earth Planet. Inter.*, *54*(1–2), 120–134, 1989.

Ehlers, T. A., and D. S. Chapman, Normal fault thermal regimes; conductive and hydrothermal heat transfer surrounding the Wasatch Fault, Utah, *Tectonophysics*, *312*(2–4), 217–234, 1999.

Ehlers, T. A., P. A. Armstrong, and D. S. Chapman, Normal fault thermal regimes and the interpretation of low-temperature thermochronometers, in *Thermal Studies of the Earth's Structure and Geodynamics*, edited by I. T. Kukkonen, V. Cermak, and B. Kennett, pp. 179–194, Elsevier Sci., New York, 2001.

Elsasser, W. M., Convection and stress propagation in the upper mantle, in *The Application of Modern Physics to the Earth and Planetary Interiors*, edited by S. K. Runcorn, pp. 223–246, Wiley-Interscience, New York, 1969.

Flesch, L. M., W. E. Holt, A. J. Haines, and B. Shen-Tu, Dynamics of the Pacific-North American plate boundary in the western United States, *Science*, *287*, 834–836, 2000.

Foulger, G. R., C. H. Jahn, G. Seeber, P. Einarsson, B. R. Julian, and K. Heki, Post-rifting stress relaxation at the divergent plate boundary in northeast Iceland, *Nature*, *358*(6386), 488–490, 1992.

Gans, P. B., and W. A. Bohrson, Suppression of volcanism during rapid extension in the Basin and Range Province, United States, *Science*, *279*, 66–68, 1998.

Grant, L., and K. Sieh, Paleoseismic evidence of clustered earthquakes on the San Andreas fault in the Carrizo Plain, California, *J. Geophys. Res.*, *99*, 6819–6841, 1994.

Hager, B. H., G. A. Lyzenga, A. Donnellan, and D. Dong, Reconciling rapid strain accumulation with deep seismogenic fault planes in the Ventura Basin, California, *J. Geophys. Res.*, *104*, 25,207–25,219, 1999.

Handwerger, D. A., T. E. Cerling, and R. L. Bruhn, Cosmogenic ^{14}C in carbonate rocks, *Geomorphology*, *27*, 13–24, 1999.

Hanson, K., Fault evaluation study and seismic hazard assessment, private fuel storage facility, Skull Valley, Utah, report, Geomatrix Consultants, Inc., San Francisco, Calif., 1999.

Hecker, S., Quaternary tectonics of Utah with emphasis on earthquake-hazard characterization, *Bull. Utah Geol. Surv.*, *127*, 157 pp., 1993.

Helm, J. M., Quaternary faulting in the Stansbury fault zone, Tooele County, UT, in *Environmental and Engineering Geology of the Wasatch Front Region*, edited by W. R. Lund, pp. 31–44, Utah Geol. Assoc., Salt Lake City, 1995.

Imbrie, J., et al., The orbital theory of Pleistocene climate: Support from a revised chronology of the marine delta18 O record, in *Milancovitch and Climate (Part 1)*, edited by A. L. Berger et al., pp. 269–305, D. Reidel, Norwell, Mass., 1984.

Izett, G. A., and R. E. Wilcox, Map showing localities and inferred distributions of the Huckleberry Ridge, Mesa Falls, and Lava Creek ash beds (Pearlette family ash beds) of Pleistocene age in the western United States and southern Canada, *U.S. Geol. Surv. Misc. Invest. Ser. Map, I-1325*, 1 sheet, 1982.

John, A. D., Geologic setting, depths of emplacement, and regional distribution of fluid inclusions in intrusions of the central Wasatch Mountains, Utah, *Econ. Geol.*, *84*, 386–409, 1989.

Keaton, J. R., D. R. Currey, and S. J. Olig, Paleoseismicity and earthquake hazard evaluation of the West Valley fault zone, Salt Lake City urban area, Utah, report, Dames and Moore, Salt Lake City, 55 pp., 1987.

Kenner, S. J., and P. Segall, A mechanical model for intraplate earthquakes: Application to the New Madrid seismic zone, *Science*, *289*, 2329–2332, 2000.

Kowallis, B. J., J. Ferguson, and G. J. Jorgensen, Uplift along the Salt Lake segment of the Wasatch Fault from apatite and zircon fission track dating in the Little Cottonwood Stock, in *Proceedings of the 6th International Fission Track Dating Workshop*, edited by S. A. Durrani and E. V. Benton, pp. 325–329, Pergamon, New York, 1990.

Langbein, J. L., F. Wyatt, H. Johnson, D. Hamann, and P. Zimmer, Improved stability of a deeply anchored geodetic monument for deformation monitoring, *Geophys. Res. Lett.*, *22*, 3533–3536, 1995.

Lee, J.-J., and R. L. Bruhn, Structural anisotropy of normal fault surfaces, *J. Struct. Geol.*, *18*(8), 1043–1059, 1996.

Lund, W. R., (Ed.), The Oquirrh Fault Zone, Tooele County, Utah; surficial geology and paleoseismicity, in *Paleoseismology of Utah*, vol. 6, *Spec. Study 88*, p. 94, Utah Geol. Surv., Salt Lake City, 1996.

Machette, M. N., Preliminary investigations of late Quaternary slip rates along the southern part of the Wasatch fault zone, central Utah, in *Proceedings of Conference XXVI; A Workshop on Evaluation of Regional and Urban Earthquake Hazards and Risk in Utah*, *Conference XXVI*, edited by W. W. Hays and P. L. Gori, *U.S. Geol. Surv. Prof. Pap.*, *1275*, 391–406, 1981.

Machette, M. N., and M. N. Machette, Late Cenozoic geology of the Beaver Basin, southwestern Utah, *Geol. Stud. 32,* pp. 19–37, Brigham Young Univ., Provo, Utah, 1985.

Machette, M. N., S. F. Personius, and A. R. Nelson, The Wasatch fault zone, Utah-segmentation and history of holocene earthquakes, *J. Struct. Geol.*, *13*(2), 137–149, 1991.

Machette, M. N., S. F. Personius, and A. R. Nelson, The Wasatch Fault Zone, U.S.A., *Ann. Tectonophys.*, *6*, 5–39, 1992a.

Machette, M. N., S. F. Personius, and A. R. Nelson, Paleoseismology of the Wasatch fault zone—A summary of recent investigations, conclusions, and interpretations, in *Assessing Regional Earthquake Hazards and Risk Along the Wasatch Front*, *Utah*, edited by P. A. Gori and W. W. Hays, *U.S. Geol. Surv. Prof. Pap.*, *1500*, A1–A72, 1992b.

Madsen, D. B., and D. R. Currey, Late Quaternary glacial and vegetation changes, Little Cottonwood Canyon area, Wasatch Mountains, Utah, *Quat. Res.*, *12*(2), 254–268, 1979.

Marco, S., M. Stein, A. Agnon, and H. Ron, Long-term earthquake clustering: A 50,000-year paleoseismic record in the Dead Sea Graben, *J. Geophys. Res.*, *101*, 6179–6191, 1996.

Martinez, L. J., C. M. Meertens, and R. B. Smith, Rapid deformation rates along the Wasatch fault zone, Utah, from first GPS measurements with implications for earthquake hazard, *Geophys. Res. Lett.*, *25*, 567–570, 1998.

Mattson, A., and R. L. Bruhn, Nonlinear diffusion-equation modeling of Quaternary fault morphology: Wasatch fault zone and eastern Great Basin, *J. Geophys. Res.*, *106*, 13,739–13,750, 2001.

McCalpin, J., New age control from the Wasatch fault megatrench of 1999, *Geol. Soc. Am. Abstr. Programs*, *34*(4), A12, 1999.

McCalpin, J. P., and M. E. Berry, Soil catenas to estimate ages of movements on normal fault scarps, with an example from the Wasatch fault zone, Utah, USA, *Catena*, *27*(3–4), 265–286, 1996.

McCalpin, J., and C. Nelson, Long recurrence records from the Wasatch Fault, Utah, NEHRP Annual Report, 61 pp., U.S. Geol. Surv., Reston, Va., 2000.

McCalpin, J., and S. Nishenko, Holocene paleoseismicity, temporal clustering, and probabilities of future large ($M > 7$) earthquakes on the Wasatch fault zone, Utah, *J. Geophys. Res.*, *101*, 6233–6253, 1996.

Moore, M. A., and P. C. England, On the inference of denudation rates from cooling ages of minerals, *Earth Planet. Sci. Lett.*, *185*(3–4), 265–284, 2001.

Nelson, A. R., Lithofacies analysis of colluvial sediments; an aid in interpreting the Recent history of Quaternary normal faults in the Basin and Range Province, western United States, *J. Sediment. Petrol.*, *62*(4), 607–621, 1992.

Niemi, N. A., B. P. Wernicke, A. M. Friedrich, R. A. Bennett, and J. L. Davis, BARGEN continuous GPS data across the eastern Basin and Range Province and implications for fault system dynamics, *Geophys. J. Int.*, in press, 2003.

Olig, S. S., W. R. Lund, B. D. Black, and M. Morisawa, Large mid-Holocene and late Pleistocene earthquakes on the Oquirrh fault zone, Utah: Geomorphology and natural hazards, *Geomorphology*, *10*(1–4), 285–315, 1994.

Olig, S. S., W. R. Lund, B. D. Black, and B. H. Mayes, Paleoseismic investigations of the Oquirrh Fault zone, Tooele County, Utah, in The Oquirrh fault zone, Tooele County, Utah: Surficial geology and paleoseismicity, in *Paleoseismology of Utah*, vol. 6, *Spec. Study 88*, pp. 22–64, Utah Geol. Surv., Salt Lake City, 1996.

Oviatt, C. G., and W. D. McCoy, Stop 1; The Cutler Dam Alloformation; deposits of a probable early Wisconsin lake in the Bonneville Basin, in *In*

the Footsteps of G.K. Gilbert; Lake Bonneville and Neotectonics of the Eastern Basin and Range Province: Geological Society of America Guidebook for Field Trip Twelve, edited by M. N. Machette, *Misc. Publ. 88-1*, pp. 20–26, Utah Geol. and Mineral. Surv., Salt Lake City, 1988.

Oviatt, C. G., D. R. Currey, and D. Sack, Radiocarbon chronology of Lake Bonneville, eastern Great Basin, USA, *Palaeogeogr. Palaeoclimatol. Palaeoecol.*, *99*(3–4), 225–241, 1992.

Parry, W. T., and R. L. Bruhn, Pore fluid and seismogenic characteristics of fault rock at depth on the Wasatch Fault, Utah, *J. Geophys. Res.*, *91*, 730–744, 1986.

Parry, W. T., and R. L. Bruhn, Fluid inclusion evidence for minimum 11 km vertical offset on the Wasatch Fault, Utah, *Geology*, *15*(1), 67–70, 1987.

Pechmann, J. C., W. P. Nash, J. J. Viveiros, and R. B. Smith, Anonymous, Slip rate and earthquake potential of the East Great Salt Lake Fault, Utah, *Eos Trans. AGU*, *68*, 1369, 1987.

Phillips, F. M., and M. A. Plummer, Anonymous, Late Pleistocene glacial/lacustrine correlations across the Great Basin from Bonneville to the Sierra Nevada, *Geol. Soc. Am. Abstr. Programs*, *29*(6), 254–255, 1997.

Reid, H. F., The California earthquake of April 18, 1906, The mechanics of the earthquake, Report of the (California) State Earthquake Investigation Commission, vol. 2, *Publ. 87*, pp. 1–192, Calif. State Earthquake Invest. Comm., Sacramento, 1910.

Richmond, G. M., Stratigraphy and correlation of glacial deposits of the Rocky Mountains, the Colorado Plateau and the ranges of the Great Basin, Quaternary glaciations in the Northern Hemisphere, *Quat. Sci. Rev.*, *5*, 99–127, 1986.

Rockwell, T., S. Lindvall, M. Herzberg, D. Murbach, T. Dawson, and G. Berger, Paleoseismology of the Johnson Valley, Kickapoo, and Homestead Valley faults: Clustering of earthquakes in the eastern California shear zone, *J. Geophys. Res.*, *90*, 1200–1236, 2000.

Ruppel, C., L. Royden, and K. V. Hodges, Thermal modeling of extensional tectonics; application to pressure-temperature-time histories of metamorphic rocks, *Tectonics*, *7*(5), 947–957, 1988.

Savage, J. C., Viscoelastic-coupling model for the earthquake cycle driven from below, *J. Geophys. Res.*, *105*, 25,525–25,532, 2000.

Savage, J. C., and R. O. Burford, Geodetic determination of relative plate motion in central California, *J. Geophys. Res.*, *78*, 832–845, 1973.

Savage, J. C., M. Lisowski, and W. H. Prescott, Strain accumulation across the Wasatch Fault near Ogden, Utah, *J. Geophys. Res.*, *97*, 2071–2083, 1992.

Scholz, C., *The Mechanics of Earthquakes and Faulting*, 461 pp., Cambridge Univ. Press, New York, 1990.

Schwartz, D. P., and K. J. Coppersmith, Fault behavior and characteristic earthquakes: Examples from the Wasatch and San Andreas fault zones, *J. Geophys. Res.*, *89*, 5681–5698, 1984.

Schwartz, D. P., and W. R. Lund, Paleoseismicity and earthquake recurrence at Little Cottonwood Canyon, Wasatch fault zone, Utah, in *In the Footsteps of G.K. Gilbert; Lake Bonneville and Neotectonics of the Eastern Basin and Range Province: Geological Society of America Guidebook for Field Trip Twelve*, edited by M. N. Machette, *Misc. Publ. 88-1*, pp. 82–85, Utah Geol. and Mineral. Surv., Salt Lake City, 1988.

Schwartz, D. P., K. Hanson, and F. H. Swan, Paleoseismic investigations along the Wasatch fault zone—An update, in *Geologic Excursions in Neotectonics and Engineering Geology in Utah, Guidebook, Part IV*, edited by K. D. Gurgel, *Spec. Stud. 59*, pp. 45–48, Utah Geol. Mineral. Surv., Salt Lake City, 1983.

Scott, W. E., Temporal relations of Lacustrian and glacial events at Little Cottonwood and Bells Canyons, Utah, in *In the Footsteps of G.K. Gilbert; Lake Bonneville and Neotectonics of the Eastern Basin and Range Province: Geological Society of America Guidebook for Field Trip Twelve*, edited by M. N. Machette, *Misc. Publ. 88-1*, pp. 86–88, Utah Geol. and Mineral. Surv., Salt Lake City, 1988.

Scott, W. E., and R. R. Shroba, Surficial geologic map of an area along the Wasatch fault zone in the Salt Lake valley, Utah, *U.S. Geol. Surv. Open File Rep., 85-448*, pamphlet, 2 plates, scale 1:24,000, 1985.

Scott, W. E., W. D. McCoy, R. R. Shroba, and M. Rubin, Reinterpretation of the exposed record of the last two cycles of Lake Bonneville, western United States, *Quat. Res.*, *20*(3), 261–285, 1983.

Shimazaki, K., and T. Nakata, Time-predictable recurrence model for large earthquakes, *Geophys. Res. Lett.*, *7*, 279–282, 1980.

Sieh, K., M. Stuiver, and D. Brillinger, A more precise chronology of earthquakes produced by the San Andreas fault in southern California, *J. Geophys. Res.*, *94*, 603–623, 1989.

Smith, R. B., and R. L. Bruhn, Intraplate extensional tectonics of the eastern Basin-Range: Inferences on structural style from seismic reflection data, regional tectonics, and thermal-mechanical models of brittle-ductile deformation, *J. Geophys. Res.*, *89*, 5733–5762, 1984.

Smith, R. B., and M. L. Sbar, Contemporary tectonics and seismicity of the western United States with emphasis of the Intermountain Seismic Belt, *Geol. Soc. Am. Bull.*, *85*, 1205–1218, 1974.

Solomon, B. J., New evidence for the age of faulting on the West Valley fault zone, *Surv. Notes 30*(3), pp. 8, 13, Utah Geol. Surv., Salt Lake City, 1998.

Sonder, L. J., and C. H. Jones, Western United States extension; how the west was widened, *Annu. Rev. Earth Planet. Sci.*, *27*, 417–462, 1999.

Stockli, D. F., Regional timing and spatial distribution of Miocene extension in the northern Basin and Range province, Ph.D. thesis, 239 pp., Stanford Univ., Stanford, Calif., 2000.

Swan, F. H., Temporal clustering of paleoseismic events on the Oued Fodda Fault, Algeria, *Geology*, *16*(12), 1092–1095, 1988.

Swan, F. H., III, D. P. Schwartz, and L. S. Cluff, Recurrence of moderate to large magnitude earthquakes produced by surface faulting on the Wasatch fault zone, Utah, *Bull. Seismol. Soc. Am.*, *70*(5), 1431–1462, 1980.

Thatcher, W., G. R. Foulger, B. R. Julian, J. Svarc, E. Quilty, and G. W. Bawden, Present-day deformation across the Basin and Range province, western United States, *Science*, *283*, 1714–1718, 1999.

Viveiros, J. J., Cenozoic tectonics of the Great Salt Lake for seismic reflection data, Master's thesis, 81 pp., Univ. of Utah, Salt Lake City, 1986.

Wallace, R. E., Patterns and timing of late Quaternary faulting in the Great Basin province and relation to some regional tectonic features, *J. Geophys. Res.*, *89*, 5763–5769, 1984.

Wallace, R. E., Grouping and migration of surface faulting and variation in slip rates on faults in the Great Basin province, *Bull. Seismol. Soc. Am.*, *77*, 868–877, 1987.

Ward, S. N., On the consistency of earthquake moment rates, geological fault data, and space geodetic strain: The United States, *Geophys. J. Int.*, *134*, 172–186, 1998.

Wernicke, B., and G. J. Axen, On the role of isostasy in the evolution of normal fault systems, *Geology*, *16*(9), 848–851, 1988.

Wernicke, B., and J. K. Snow, Cenozoic tectonism in the central Basin and Range: Motion of the Sierran-Great Valley Block, *Int. Geol. Rev.*, *40*(5), 403–410, 1998.

Wernicke, B., A. M. Friedrich, N. A. Niemi, R. A. Bennett, and J. L. Davis, Dynamics of plate boundary fault systems from Basin and Range Geodetic Network (BARGEN) and Geologic Data, *GSA Today*, *10*(11), 1–7, 2000.

Witkind, I. J., Reactivated faults north of Hebgen Lake, in *The Hebgen Lake, Montana, earthquake of August 17, 1959, U.S. Geol. Surv. Prof. Pap., 0435*, 37–50, 1964.

Zoback, M. L., R. E. Anderson, G. A. Thompson, F. J. Vine, and A. G. Smith, Cainozoic evolution of the state of stress and style of tectonism of the Basin and Range Province of the Western United States, in *Extensional Tectonics Associated With Convergent Plate Boundaries*, pp. 407–434, R. Soc. of London, London, 1981.

Zreda, M., and J. Noller, Ages of prehistoric earthquakes revealed by cosmogenic chlorine-36 in a bedrock fault scarp at Hebgen Lake, *Science*, *282*, 1097–1099, 1998.

R. A. Bennett and J. L. Davis, Smithsonian Astrophysical Observatory, Harvard University, 60 Garden Street, MS 42, Cambridge, MA 02138, USA. (rbennett@cfa.harvard.edu; jdavis@cfa.harvard.edu)

A. M. Friedrich, Institute of Geosciences, Potsdam University, Karl-Liebknechtstr. 24/Haus 25, D-14476 Golm, Germany. (anke@alum.mit.edu)

N. A. Niemi, Institute for Crustal Studies, University of California, Santa Barbara, CA 93106, USA. (niemi@crustal.ucsb.edu)

B. P. Wernicke, Division of Geological and Planetary Sciences, California Institute of Technology, 100-23 Caltech, Pasadena, CA 91125, USA. (brian@gps.caltech.edu)